Controls on pore geometry in the Tirrawarra Sandstone reservoir, Cooper Basin, Australia

Mohammad R. Rezaee[1] and N. M. Lemon[1]

Key words:
Pore geometry, depositional and diagenetic control, image analysis, mercury injection.

Abstract

Petrographic observations of 130 Tirrawarra Sandstone samples in the Moorari and Fly Lake Fields of the Cooper Basin, reveal that they can be partitioned into eight classes based on porosity type and texture. Pore spaces grade from dominantly macroporosity to dominantly microporosity from Class 1 to Class 8 samples. Pore area, size of pore throats and pore diameter, determined by image analysis and mercury injection capillary pressure data, are different for each class. Pore geometry is largely controlled by rock parameters such as composition, cementation and compaction. These parameters are, in turn, controlled by depositional environment and each class is limited to certain depositional environments. Class one samples, associated with meander, aeolian or beach-barrier environments, have primary macroporosity with partial quartz cement. Pore throats usually exceed 10 microns, mean pore space area is about 36000 micron^2 and mean pore diameter and mean pore perimeter are 170 and 350 microns respectively. At the other end of the scale, Class 8, associated with a braid-delta environment, is dominated by microporosity and has a mean pore space area of about 430 micron^2 with mean pore diameter and mean pore perimeter 24 and 75 microns respectively. The pore throat distribution shows poor sorting, ranging from 0.1 to 0.5 microns.

Introduction

Reservoir properties such as porosity and permeability are controlled by the size and arrangement of pores and pore throats (Wardlaw 1976; McCreesh et al. 1991; Pittman 1992; Ehrenberg & Boassen 1993). Detailed study of pore geometry is needed to give a better understanding of reservoir rocks and how they are likely to perform during production. To find possible new ways to predict pore geometry of reservoir formations, the factors which control pore geometry (depositional fabrics or/and post depositional events) should also be quantitatively studied. Petrographic image analysis procedures (Ehrlich et al. 1984; Ehrlich et al. 1991) enable the quantitative evaluation of characteristics such as pore surface area, pore diameter and pore perimeter. Mercury injection (Purcell, 1949) can provide the pore throat sizes of the samples.

The role of diagenetic events on pore geometry is indicated by many workers (e.g. Pittman 1979; Tingate & Luo 1992) and several workers in the Cooper Basin have studied the influence of diagenetic events on the porosity and permeability of the Permian reservoir rocks (Farrow 1989; Schulz-Rojahn & Phillips 1989; Stuart et al. 1990). There is, however, a lack of a quantitative approach in the literature to evaluate the influence of depositional environments and post-depositional events on the pore geometry in sandstone reservoirs.

In the present work, pore space characteristics of the Tirrawarra Sandstone were evaluated with petrographic image analysis and mercury injection to indicate the size and distribution of pore throats. These data were then integrated with petrographic point-counts, depositional facies information and core porosity and permeability values. The results show that, in the Tirrawarra Sandstone, depositional facies influence sandstone texture and composition, and composition controls diagenetic events such as mechanical compaction and cementation which in turn control pore geometry.

Geologic setting

The Late Carboniferous-Triassic Cooper Basin of central Australia (Fig. 1) is a major hydrocarbon province (Hunt et al. 1989) underlain by Early Paleozoic marine and volcanic rocks of the Warburton Basin (Gatehouse, 1986) and overlain by Jurassic-Cretaceous sediments of the Eromanga Basin (Exon & Senior, 1976; Senior et al., 1978; Armstrong & Barr, 1986). Basin fill, having a maximum thickness of 1300 m, consists dominantly of lacustrine-fluvial deposits with local glacio-fluvial and rare paraglacial aeolian sediments (Kapel, 1966, 1972; Gatehouse, 1972; Battersby, 1976; Thornton, 1979; Stuart, 1976; Williams et al., 1985; Fairburn, 1989). Cooper Basin deposition terminated at the end of the Early-Mid Triassic when widespread

[1] National Centre for Petroleum Geology & Geophysics, Adelaide, South Australia.

Forrest, J.T. and Horstman, E.L., 1986, The Northwest Shelf of Australia - geologic review of a potential major petroleum province of the future. AAPG Memoir, 40, pp. 457-486.

Gorter, J.D., 1994, Triassic sequence stratigraphy of the Carnarvon Basin, Western Australia. *In:* Purcell, P.G. and R.R., (eds), The sedimentary basins of Western Australia. Petroleum Exploration Society of Australia, Perth. 1994. pp. 379-414.

Gunn, P.J. and Ly, K.C., 1989, The petroleum prospectivity of the Joseph Bonaparte Gulf area, northwestern Australia. APEA Journal, vol. 29, pt. 1, pp. 509-526.

Hill, G., 1994, The role of the pre-rift structure in the architecture of the Dampier Basin area, North West Shelf, Australia. APEA Journal, vol. 34, part. 1, pp. 602-613.

Hocking, R.M., Moors H.T. and van de Graaff, W.J.E., 1987, The geology of the Carnarvon Basin, W.A. Geological Survey of Western Australia, Bulletin 133.

Hocking, R.M., 1988, Regional geology of the Northern Carnarvon Basin: *In:* Purcell, P.G. and R.R., (eds), The North West Shelf, Australia. Petroleum Exploration Society of Australia, Perth. 1988. pp. 97-114.

Hocking, R.M., 1990, Carnarvon Basin. *In:* Geology and Mineral Resources of Western Australia: Geological Survey of Western Australia, Memoir 3, pp. 457-495.

Hocking, R.M., 1994, Subdivisions of Western Australian Neoproterozoic and Phanerozoic sedimentary basins. Geological Survey of Western Australia Report, 1994/4.

Hocking, R.M., Mory, A.J. and Williams, I.R., 1994, An atlas of Neoproterozoic and Phanerozoic basins of Western Australia. *In:* Purcell, P.G. and R.R. (eds), The sedimentary basins of Western Australia. Petroleum Exploration Society of Australia symposium, Perth. 1994. pp. 21-44.

Kingston, D.R., Dishroon, C.P. and Williams, P.A., 1983, Global basin classification system. AAPG Bulletin, vol. 67, no. 12, pp. 2175-2193.

Kirk, R.B., 1985, A seismic stratigraphic case history in the eastern Barrow Sub-basin, North West Shelf, Australia: *In:* Berg, O.R. and Woolverton, D., (eds), Seismic stratigraphy - II: AAPG Memoir, 39, pp. 183-207.

Kopsen, E. and McGann, G., 1985, A review of the hydrocarbon habitat of the eastern and central Barrow-Dampier sub-basin, Western Australia. APEA Journal, vol. 25, pt. 1, pp. 154-176.

Mahmood, T., 1996, Three dimensional analogue modelling of extensional fault systems and application to the Barrow - Dampier Sub-basin, Western Australia. University of Adelaide, Ph.D thesis (unpublished).

Metcalfe, I., 1988, Origin and assembly of south-east Asian continental terranes. *In:* Audley-Charles, M.G. and Hallam, A., (eds), Gondwana and Tethys: Geological Society Special Publication no. 37, pp. 101-118.

Metcalfe, I., 1993, Southeast Asian terranes: Gondwanaland origins and evolution. *In:* Findlay, Unrug, Banks & Veevers, (eds), Gondwana Eight: A.A. Balkema, Rotterdam, pp. 181-200.

O'Brien, G.W., Etheridge, M.A., Willcox, J.B., Morse, M., Symonds, P., Norman, C., and Needham, D.J., 1993, The structural architecture of the Timor Sea, north-western Australia: implications for basin development and hydrocarbon exploration: APEA Journal, 1993, vol. 33, pt. 1, pp. 258-278.

Polomka, S.M., 1996, Development from rift to passive margin: structure and sedimentology. A case study from the Barrow Sub-basin: University of South Australia, Ph.D thesis (unpublished).

Quaife, P., Rosser, J. and Pagnozzi, S., 1994, The structural architecture and stratigraphy of the offshore northern Perth Basin, Western Australian. *In:* Purcell, P.G. and R.R. (eds), The sedimentary basins of Western Australia. Petroleum Exploration Society of Australia, Perth. 1994. pp. 812-822.

Rosendahl, B.R., Reynolds, D.J., Lorber, P.M., Burgess, C.F., McGill, J., Scott, D., Lambiase, J.J. and Derksen, S.J., 1986, Structural expressions of rifting: lessons from Lake Tanganyika, Africa. *In:* Frostick, L.E., Renaut, W.R., Reid, I. & Tiercelin, J.J., (eds), Sedimentation in the African rifts, Geological Society Special Publication, no. 25, pp. 29-43.

Selley, R.C., 1988, Applied sedimentology. Academic Press, London, pp. 466.

Stagg, M.J. and Colwell, J.B., 1994, The structural foundations of the northern Carnarvon Basin. *In:* Purcell, P.G. and R.R., (eds), The Sedimentary Basins of Western Australia. Petroleum Exploration Society of Australia, Perth. 1994. pp. 349-364.

Veevers, J.J., 1988, Morphotectonics of Australia's northwestern margin. *In:* Purcell P.G. and R.R., (eds), The North West Shelf, Australia. Petroleum Exploration Society of Australia, Perth. 1988. pp 19-27.

Woodside Offshore Petroleum, 1988, Petroleum geology and hydrocarbon potential of the Barrow-Dampier Sub-basin and environs. Petroleum in Australia, the First Century: Australian Petroleum Exploration Association, pp. 213-231.

Yeates, A.N., Bradshaw, M.T., Dickins, J.M., Brakel, A.T., Exon, N.F., Langford, R.P., Mulholland, S.M., Totterdell, J.M. and Yeung, M., 1987, The Westralian Superbasin: an Australian link with Tethys. *In:* McKenzie, K.G., (ed), Shallow Tethys 2: A.A. Balkema, Rotterdam, pp. 199-213.

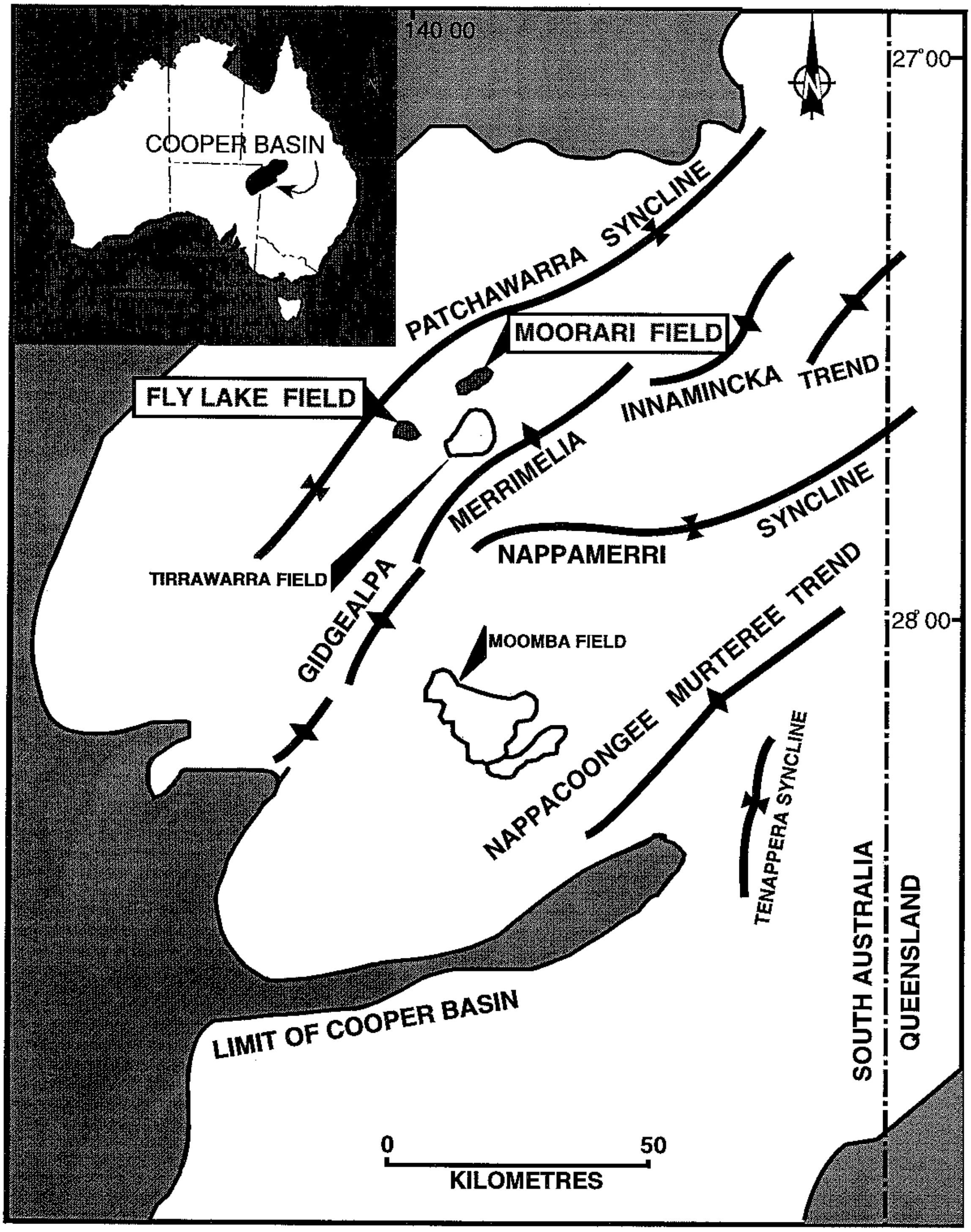

Fig. 1 - Map of the southern Cooper Basin showing major structural elements; modified from Stuart et al. (1988).

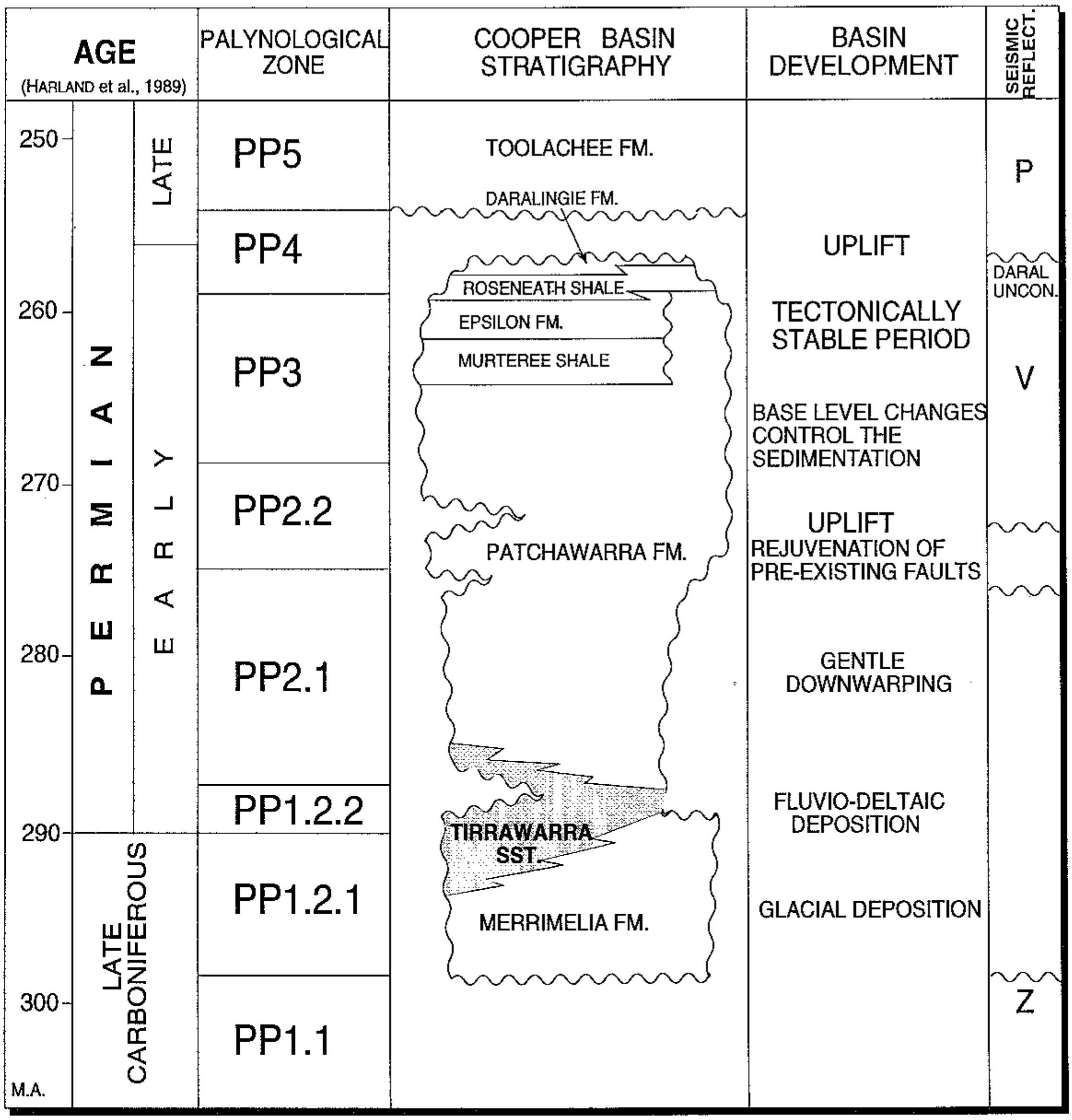

Fig. 2 - Stratigraphic column for the southern Cooper Basin; modified from Apak et al. (1993) and Seggie et al. (1994).

compressional folding, regional uplift and erosion occurred (Battersby, 1976). Rejuvenation of pre-Permian faults along the flanks of many structures occurred contemporaneously with Cooper Basin deposition (Battersby, 1976; Stuart, 1976; Apak et al., 1993). Fluvial sandstones, which occur at various levels within the Permian section, represent the main petroleum reservoirs, including the fluvio-glacial Tirrawarra Sandstone (Smyth, 1979; Kantsler et al., 1983; Heath, 1989; Hunt et al., 1989; Yew & Mills, 1989). About 95% of the Cooper Basin oil is reservoired in the Tirrawarra Sandstone of the Tirrawarra Field (Heath, 1989) (Fig.2). Additional oil reserves occur at the same stratigraphic interval in the Moorari and Fly Lake Fields (Fig.1). In both fields, the Tirrawarra Sandstone reservoirs are characterised by relatively low porosities (9 to 12%), low permeabilities (0.1 to 15 md *in situ*) and hence relatively low productivities (25 to 600 BOPD) (Rodda & Paspaliaris, 1989; Yew & Mills, 1989).

Palaeoenvironmental interpretations

Various depositional environments recognised during this study in the Tirrawarra Sandstone include:

- Lacustrine (L) with upper and lower shoreface zones.
- Shoreline-parallel beach barriers (BS).
- Back barrier marshes with outwash beds (MBB).
- Distal braid-deltas with linguoid bars, inter-channel bay deposits and splays (BD).
- Medial braid-deltas with longitudinal bars (BM).
- Meandering fluvial systems (M).
- Aeolian environments (E).

The lacustrine environment consists of both upper and lower shoreface zones. The upper shoreface is dominantly very fine-to fine-grained, wave-rippled sandstones that were formed above wave base. The lower shoreface is planar-bedded, varve-like, dark mudstone with thin lenses of siltstone. Beach barrier sandstones are chiefly medium-grained, well sorted quartzarenite. They are formed by reworking of foreshore sediments by beach-parallel waves and currents. The back-barrier marsh contains massive mudstones, fine-grained sandstones and thin coal beds. They were formed in a shallow, elongate marsh landward of the barrier bar sands. The distal part of the braid-delta is dominantly composed of medium- to coarse-grained, moderately sorted sandstones with some thin intercalations of mudstone. These beds were formed as linguoid bars, in channels and in overbank areas with crevasse splays. The medial part of the braid-delta is composed of massive and crudely trough cross-bedded conglomerates and pebbly trough and planar cross-bedded, very coarse-grained, poorly-sorted sandstones, considered to have been deposited as longitudinal bars and channel fills. The meandering system is composed of matrix-supported, oligomictic lag gravel, medium-grained well-sorted point bar quartzarenite and floodplain mudstone and coal intervals. Aeolian beds are composed of thin, medium-grained, supermature quartzarenite that probably formed on the point bar sands during times of low discharge.

The vertical succession of facies associations developed during this study suggests three depositional sequences in the Tirrawarra Sandstone around the Moorari and Fly Lake Fields (Fig. 3). The vertical succession records progradation and retreat of a braid-delta into a lacustrine environment. The lower Tirrawarra Sandstone records a progradational sequence that is overlain by a retrogradational sequence then another progradation. The remaining upper part of the unit displays a sudden change in sedimentary environment from a braided to a meandering fluvial system. The boundary is marked by a thin, widespread conglomerate with an erosional lower contact which suggests a hiatus.

Methods

A total of 130 Tirrawarra Sandstone core samples was collected from 14 wells from the Moorari and Fly Lake Fields in the Cooper Basin (Fig. 1). Detailed sedimentological descriptions of the cores were carried out and a variety of lithofacies were sampled. All samples were prepared either as normal thin or polished sections following impregnation of the samples with blue-dye epoxy resin to facilitate the recognition of porosity. Quantitative estimates of sandstone mineralogy, texture and porosity were obtained by counting between 400-600 points per thin section. Approximately 100 grains were measured in each slide, using the long dimension of each grain, to estimate the mean grain size and sorting of the samples.

Scanning electron microscope (SEM) studies were carried out on selected core samples coated with carbon and gold/palladium using a Phillips XL20 electron microscope connected to a back-scattered electron (BSE) detector. Petrographic image analysis of about 66 coated polished sections was accomplished using a Phillips image analysis system in conjunction with the SEM. The BSE images of coated polished sections were imported from the SEM in the form of grey-scale binary images using a video camera and a Windows-based software programme called Image Analysis™. BSE grey images were then converted to a binary image containing only grains (white) and porosity (black). Calculation of pore parameters was accomplished by converting the analog output to a digital format.

Capillary pressures from a total of 33 representative samples were measured by mercury injection using a Micromeritics Autopore 9200 at the University of South Australia.

General diagenetic characteristics

The reservoirs of the Tirrawarra Sandstone in the Moorari and Fly Lake Fields (Fig. 1) consist mainly of medium-grained, moderately-sorted sublitharenites (Folk, 1974). Detrital modes are shown on Figure 4. Rock fragments include metamorphic, sedimentary, and volcanic types. Schists and shale are the most common rock fragments and behave in a ductile manner during compaction. The amount of rock fragments varies widely and is facies-dependent, ranging from 1.3 to 66.9 per cent (average 16.3 per cent). The amounts of quartz and rock fragments are controlled by depositional facies with each environment having a characteristic composition (Fig. 4). Apart from a few that have some heavily altered feldspar grains, most samples are almost totally lacking in recognisable feldspar grains. A number of authigenic minerals are recognised in the Tirrawarra Sandstone, including syntaxial quartz overgrowths, patchy kaolin, siderite and minor illite.

Quartz is the dominant pore-filling cement in most samples. The amount of quartz cement ranges from zero to approximately 19 per cent and is controlled by the composition of the sandstones (Rezaee & Lemon, 1996). As the percentage of rock fragments increases, the amount of quartz cement decreases (Fig. 5). Quartz cementation appears to be developed very early in some samples with a low concentration of ductile rock fragments as indicated by the preservation of the original intergranular volume (IGVo) (Fig. 6). The development of quartz cement is inhibited by

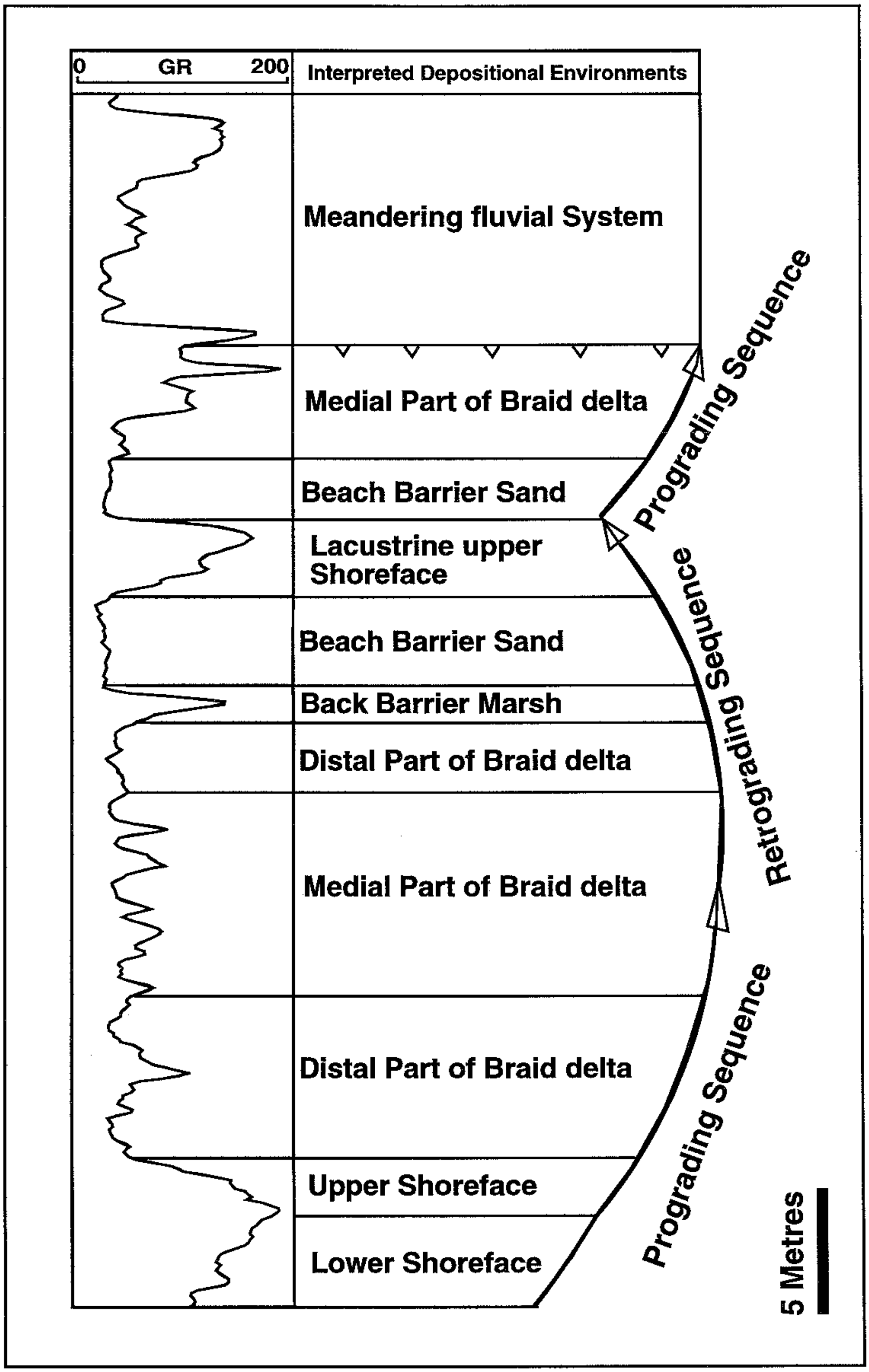

Fig. 3 - Example of the different depositional environments, and progradational and retrogradational cycles of the Tirrawarra Sandstone in the Moorari and Fly Lake Fields; gamma ray log trace is derived from the Moorari-9 well.

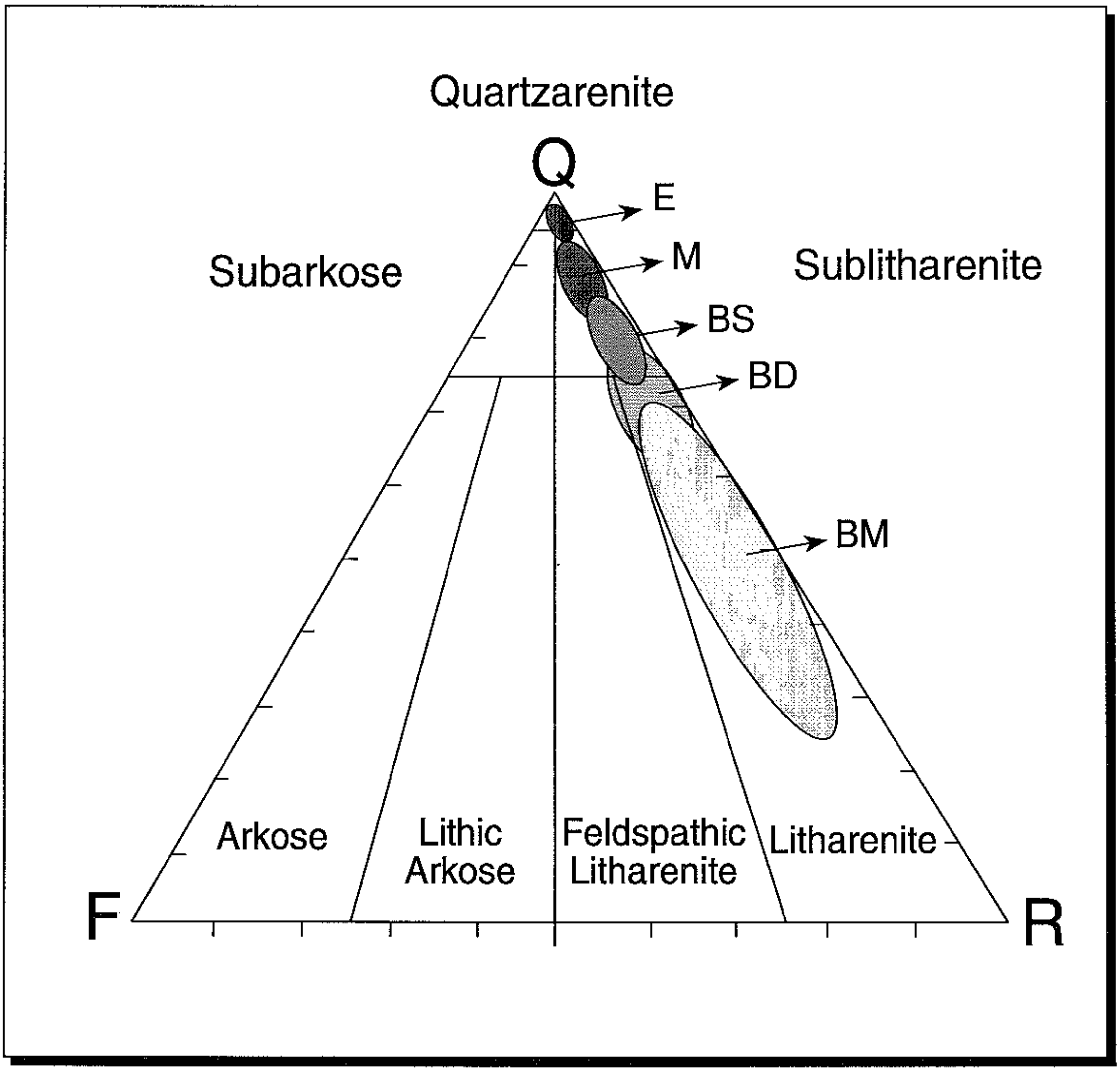

Fig. 4 - QFR ternary diagram of the Tirrawarra Sandstone; (classification after Folk, 1974). BM= medial part of braid-delta, BD= distal part of the braid-delta, BS= beach barrier, M= meandering system and E= aeolian.

the presence of any grains other than quartz. Cathodoluminesence (CL) studies indicate at least six stages of quartz cement, although three main phases are distinguished (Rezaee & Tingate, 1996, 1997). Homogenisation temperatures of fluid inclusions entrapped within the quartz cement indicate that it precipitated at temperatures between 65° and 130°C, assuming the fluid inclusions were not re-equilibrated during burial (Osborne & Haszeldine, 1993; Haszeldine & Osborne, 1993). Loose grain packing shows quartz cementation was initiated prior to the major compaction but probably continued until relatively recent times.

Two major clay mineral groups were recognised in thin-sections, and by SEM, energy dispersive X-ray (EDX) and X-ray Diffraction (XRD) analyses. Kaolin, in the form of pseudo-hexagonal stacked plates is pervasive in nearly all of the samples. Genetically, there are two kinds of authigenic kaolin in the Tirrawarra Sandstone. The first group is formed from complete replacement of the original precursor grains (most probably feldspar grains) and shows the exact margin of the original grains. The second group is directly precipitated from the pore fluids. This pore-filling cement alters the intergranular macroporosity to microporosity among the kaolin booklets. This type of kaolin, which is coarser grained than the former (about 40 microns), is often vermicular, shows less packing and intergrowth shows it to be cogenetic with quartz cement. The amount of kaolin in the samples is very variable and is also facies-dependent. Replacement kaolin ranges from 0.0 to 4.9 per cent (average 2.2 per cent) and pore-filling kaolin ranges from 0.0 to 8.1 per cent (average 3.8 per cent). BSE image analysis of the clay minerals in the Tirrawarra Sandstone using the method of Nadeau & Hurst (1990) and Hurst & Nadeau (1995) indicates a wide range of microporosity in the kaolin with the average of 20 per cent.

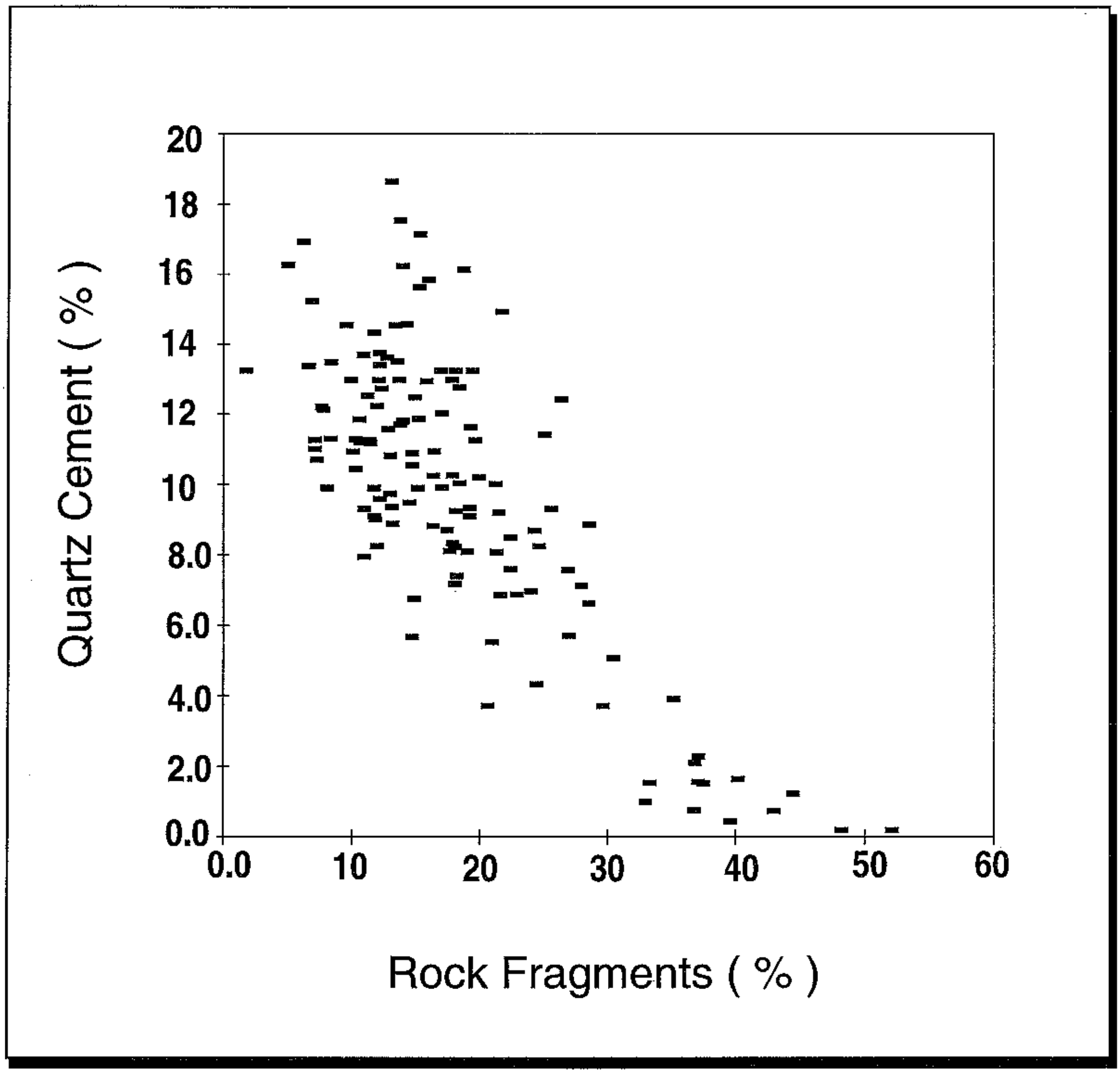

Fig. 5 - Cross-plot of rock fragment and quartz cement.

Siderite is the only carbonate cement that occurs in varying proportions in the Tirrawarra Sandstone and constitutes up to about 30 per cent of rock composition (as determined by point-counting). Siderite generally occurs as isolated, sparry rhombs or as a pore-filling cement, although a variety of different crystal habits are apparent, including rhombohedral, blocky and radial forms. Although petrographic and XRD results suggest a single-phase cement, when viewed under the electron microprobe and using BSE imaging techniques, three main stages of siderite cement are identified within the overall diagnetic history of the rock, including an early (S1), middle (S2), and late stage cement (S3) (Rezaee & Schulz-Rojahn, 1996). It appears that siderite cements in the Tirrawarra Sandstone record tectonic activity in the form of irregular growth and dissolution highlighted by compositional zoning with stages of strong dissolution (Rezaee et al., 1997)

Illite is the second most abundant clay mineral in most of the samples. The authigenic nature of the illite is evident from its rare fibrous, lath- or lettuce-like habit, largely formed as a replacement product of unstable rock fragments.

Three different types of porosity were observed in the Tirrawarra Sandstone samples. The first type, primary intergranular porosity, remains between the euhedral faces of quartz overgrowths. The second group, secondary porosity, consists of relatively large pores which are either the product of unstable grain dissolution or enlargement of porosity by dissolution of the grain margins. Very small secondary pores are also present in some rock fragments related to the dissolution of their labile components. The third type of porosity, microporosity, mainly occurs in kaolin masses and is obviously abundant in kaolin-rich

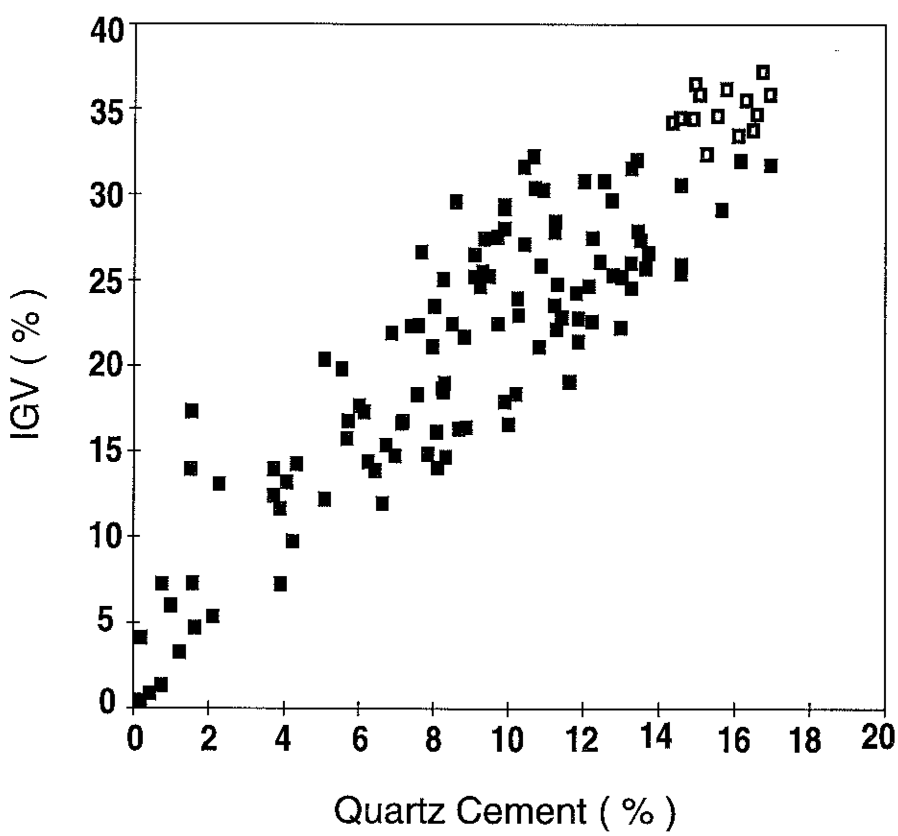

Fig. 6 - Cross-plot of quartz cement and intergranular volume (IGV).

sandstones. Larger pores of this type were termed "kaolin-framework porosity" by Luo and Tingate (1992) and were described as being significant in gas reservoirs.

Mechanical compaction is one of the most important diagenetic events controlling the reduction of intergranular porosity in the Tirrawarra Sandstone (Rezaee & Lemon, 1996). Evidence of mechanical compaction seen in thin-section includes plastic deformation of rock fragments, grain slippage and rearrangement and mica bending. In the present study, an index was employed to evaluate compaction. The Compaction Index is defined by the following equation:

$$\text{Compaction Index} = \left[\frac{IGV_o - IGV}{IGV_o}\right] * 100$$

where IGVo is original intergranular volume i.e. intergranular volume at the depositional surface and IGV is the present intergranular volume. IGVo was calculated for each sample following the method of Beard and Weyl (1973), using knowledge of sample grain size and sorting. IGV is the sum of intergranular porosity and total cement.

The magnitude of compaction in the Tirrawarra Sandstone varies from 3.1 to 95.3 per cent. Since the samples studied were all collected from reservoirs at about the same depth, the main parameters which control compaction are composition and quartz cementation. These are in turn controlled by depositional facies. As the amount of rock fragments increases, the development of quartz cement decreases (Fig. 5) and consequently compaction increases (Fig. 7).

Classification of Tirrawarra Sandstone samples

Based on petrographic observations, the Tirrawarra Sandstone samples may be assigned to eight classes according to their porosity type and texture. Class 1 contains mostly primary intergranular porosity with a successive

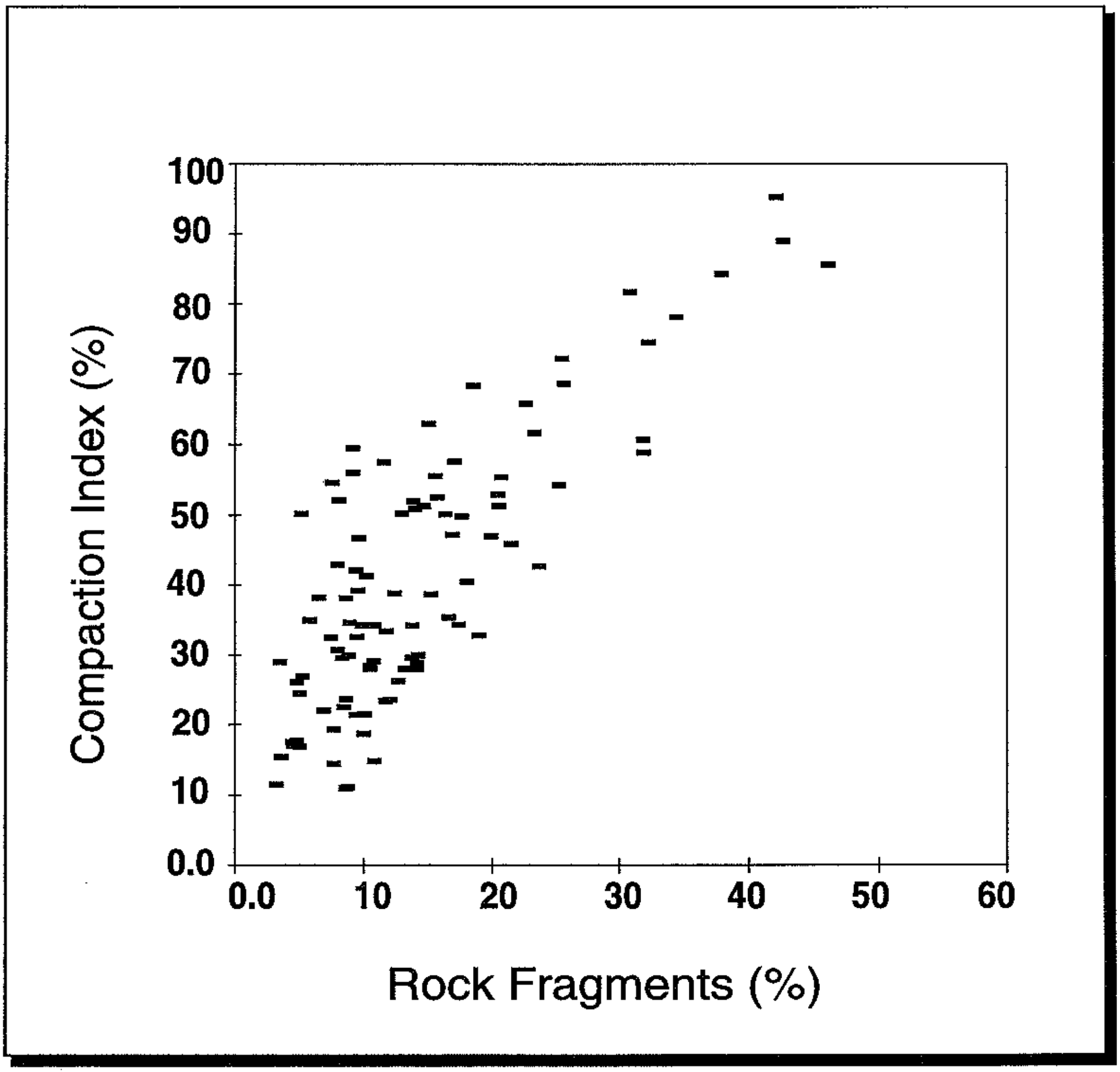

Fig. 7 - Cross-plot of rock fragment percentage and compaction index.

decrease in primary porosity towards Class 8, and a corresponding increase in the relative proportions of secondary porosity and microporosity (Figs 8a-h, 9a-h). Petrographic image analysis and mercury injection data indicate that each class has different pore space and pore throat characteristics. In general, as porosity changes from dominantly macroporosity to dominantly microporosity from Class 1 to Class 8, pore size and pore throat size decrease. The reduction of pore throat size reduces permeability. Petrographic point count data for each of the eight classes are presented in Table 1, along with average porosity and permeability data. The average pore characteristics and the dominant pore throat size of each of the eight classes is shown in Table 2.

In this classification macropores refer to any pore spaces that can be detected optically and microporosity is restricted to pore spaces among kaolin booklets.

Characteristics of classes

1 - Pore area and pore throat characteristics

Pore spaces from Class 1 to Class 8 degrade from dominantly primary intergranular porosity to isolated secondary macroporosity and microporosity associated with kaolinite (Figs 8a-h, 9a-h). The macroporosity reduces from Class 1 to Class 8 samples (Fig. 10).

Pore throats decreases from Class 1 to Class 8 (Fig. 11). The Class 1 pore throat curve displays very good sorting and in most of the cases the throat sizes are more than 10 microns, while in Class 8, the pore throat curve shows poor sorting with throat sizes mostly from 0.1 to 0.5 microns. Mean pore area, mean pore perimeter and mean pore diameter for each class are shown in Figures 12 and 13 and are summarised in Table 2.

Average Data	Class 1	Class 2	Class 3	Class 4	Class 5	Class 6	Class 7	Class 8
Core porosity (%)	14.6	11.1	13.9	11.3	9.7	13.3	10.9	7.4
Permeability (mD)	66.2	15.6	3.6	2.5	3.3	0.9	0.4	0.3
Quartz (%)	88.3	89.8	79.7	77.7	79.7	83.4	80.3	67.5
Total rock fragment (%)	11.7	10.2	20.3	22.3	20.3	16.6	19.7	32.5
Quartz cement (%)	10.5	12.1	8.9	9.2	10	10.2	10.9	6.1
Macroporosity (%)	13.3	11.6	6.7	6.4	5.4	8.3	3.8	1.7
Microporosity (%)	3.4	3.4	4.7	3.8	4.2	4.1	4.4	3.6
Total porosity (%)	16.6	14.9	11.2	10.1	9.5	12.3	8	5.2
Intergranular volume (%)	30.2	28.7	22.8	20.3	23.1	23.8	22.3	14.1
Original intergranular volume (%)	38.8	36.1	36.4	36.5	35.3	36.3	35.6	32.8
Compaction Index (%)	22.2	18.4	36.8	43	37.6	47.7	38.3	59
Grain size (mm)	0.37	0.36	0.44	0.42	0.48	0.31	0.36	0.6
Sorting (phi)	0.35	0.51	0.57	0.65	0.76	0.6	0.69	1.4

Table 1 - Averaged core porosity, permeability and point count data for each class.

	Pore area (μm²)	Pore diameter(μm)	Pore perimeter(μm)	Point-count Porosity (%)	Pore throat (μm)
Class 1	36000	210	670	13.3	>10
Class 2	30860	172	352	11.6	2
Class 3	12720	130	417	6.7	2
Class 4	7890	102	327	6.4	1.5
Class 5	2870	204	658	5.4	1.5
Class 6	343	21	57	3.7	0.2-0.7
Class 7	11240	121	396	3	0.4
Class 8	430	24	75	1.2	0.1-0.5

Table 2 - Pore area and pore throat characteristics for each class.

	Depositional Environment	Texture		Composition
		Size	Sorting	
Class 1	E & M & BS	medium-grained	well-sorted	quartzarenites
Class 2	M & BS	medium- to fine-grained	well-sorted	quartz -rich
Class 3	BS & BD	medium- to fine-grained	moderately-sorted	sublitharenites
Class 4	BS & BD & M	medium- to coarse-grained	moderately-sorted	sublitharenites
Class 5	BS & M	medium-grained	well-sorted	quartzarenites
Class 6	BD & BM & BS	medium- to fine-grained	moderately- sorted	kaolinite-rich
Class 7	BD & BM	fine-grained	poorly-sorted	litharenites
Class 8	BM	coarse to fine-grained	very poorly-sorted	litharenites

Table 3 - Depositional, textural and compositional characteristics of different classes of the Tirrawarra Sandstone.

2 - Porosity and permeability characteristics

While the porosity-permeability cross plot appears as a continuum, ambient core porosity and permeability within each class exhibit a distinct range and the samples of each class plot as a relatively distinct area on that cross plot (Fig. 14a). Samples which belong to Class 1 occupy the relatively high porosity and high permeability area, whereas Class 8 samples occupy the lowest part of the diagram in the area with low porosity and low permeability (LL). In this regard it is possible to divide Figure 14a into eight parts as HH, MH, HM, MM, LM, HL, ML, and LL (Fig. 14b). The first letter of this nomenclature refers to porosity, from relatively High (H) to Medium (M) and Low (L) and the second letter stands for permeability, from relatively High (H) to Medium (M) and Low (L), (e.g. LH refers to samples with low porosity and high permeability).

The Class 1 samples are the best parts of the Tirrawarra Sandstone reservoir and have the highest porosity and permeability (HH) and toward Class 8 (LL) porosity and permeability decrease. The average ambient core porosity and permeability for each class are summarised in Table 1.

3 - Textural and environmental characteristics

Textural maturity decreases from Class 1 towards Class 8 samples. Class 1 samples are medium-grained, well sorted and well rounded while, Class 8 samples are coarse- to fine-grained very poorly sorted sandstones. From Class 1 to Class 8, the proportion of rock fragments increases. This leads to more compaction and subsequently to more porosity loss in Class 8 samples. The low compaction of Class 1 samples is related to early quartz cement development which prevents porosity loss by providing framework support against subsequent compaction. Class 1 samples were mostly deposited in aeolian (E), meandering system (M) and beach barrier (BS) environments, whereas Class 8 samples are formed in the medial part of the braid-delta environment where the proportion of rock fragments is higher and textural maturity is less. Textural, compositional and environmental characteristics of different classes of the Tirrawarra Sandstone are summarised in Table 3.

Discussion and conclusions

Control by depositional environment on pore geometry

The results show that the occurrence of classes is limited to particular depositional environments. For example, samples of Class 1 mostly occur in aeolian (E), meandering (M) and beach barrier (BS) environments, whereas samples belonging to Class 8 occur mostly in the medial part of the braid-delta.

Each sedimentary environment is recognised by its characteristic texture, composition and diagenetic events. Reservoir quality, measured with respect to porosity and permeability, is highest in the aeolian sandstones and decreases through the meandering and beach barrier sandstones to the beds associated with the braided system (Figs 15a, b). The most likely sedimentary factors which control pore geometry, and subsequent reservoir quality, are texture and composition of the sediments.

1 - Textural characteristics of depositional environments

Texture of sand grains can have a great influence on the pore geometry and subsequently on the porosity and

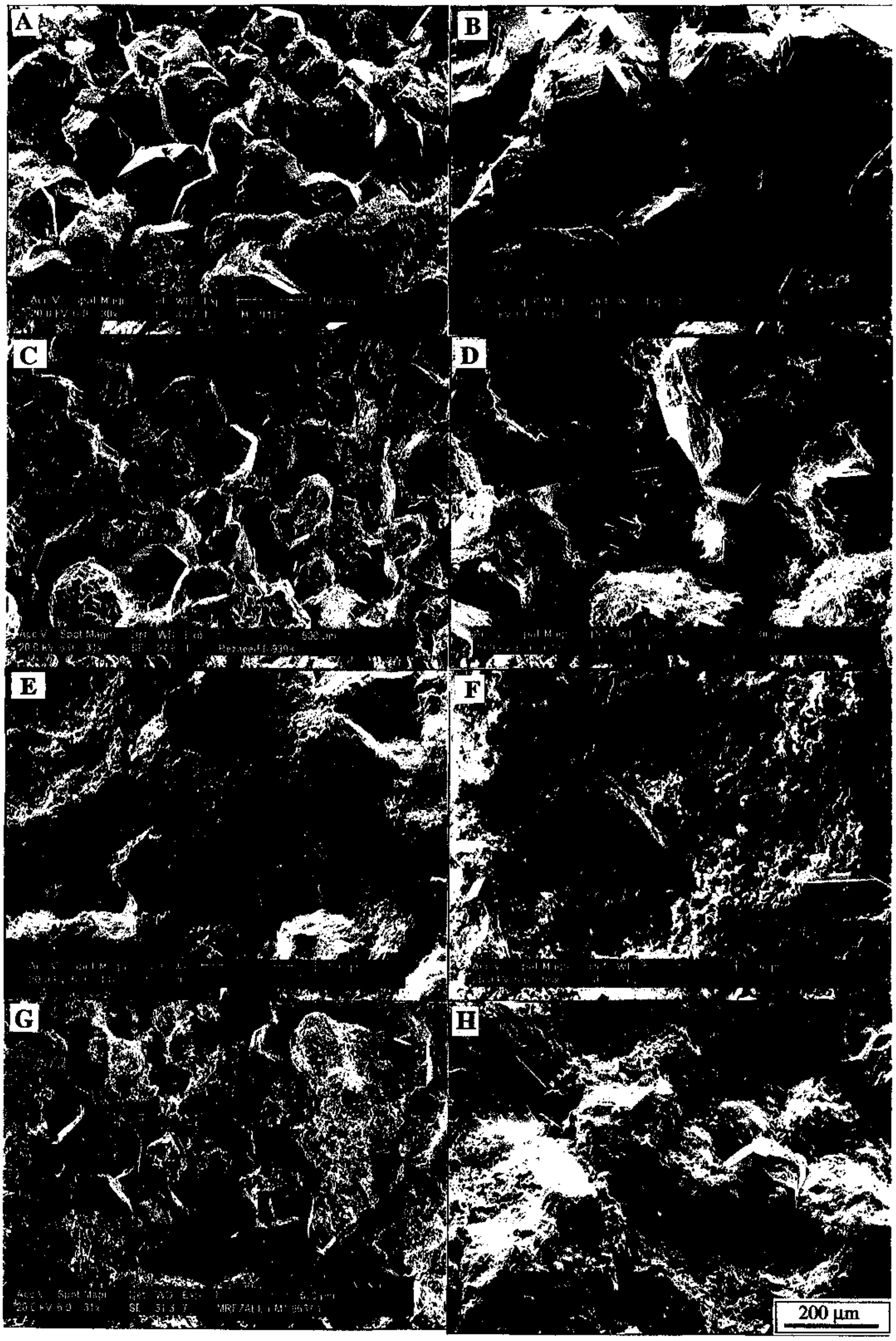

Fig. 8a-h - SEM micrographs of the representative samples of class 1 (A & B), class 2 (C & D), class 3 (E & F) and class 4 (G & H) of the Tirrawarra Sandstone.

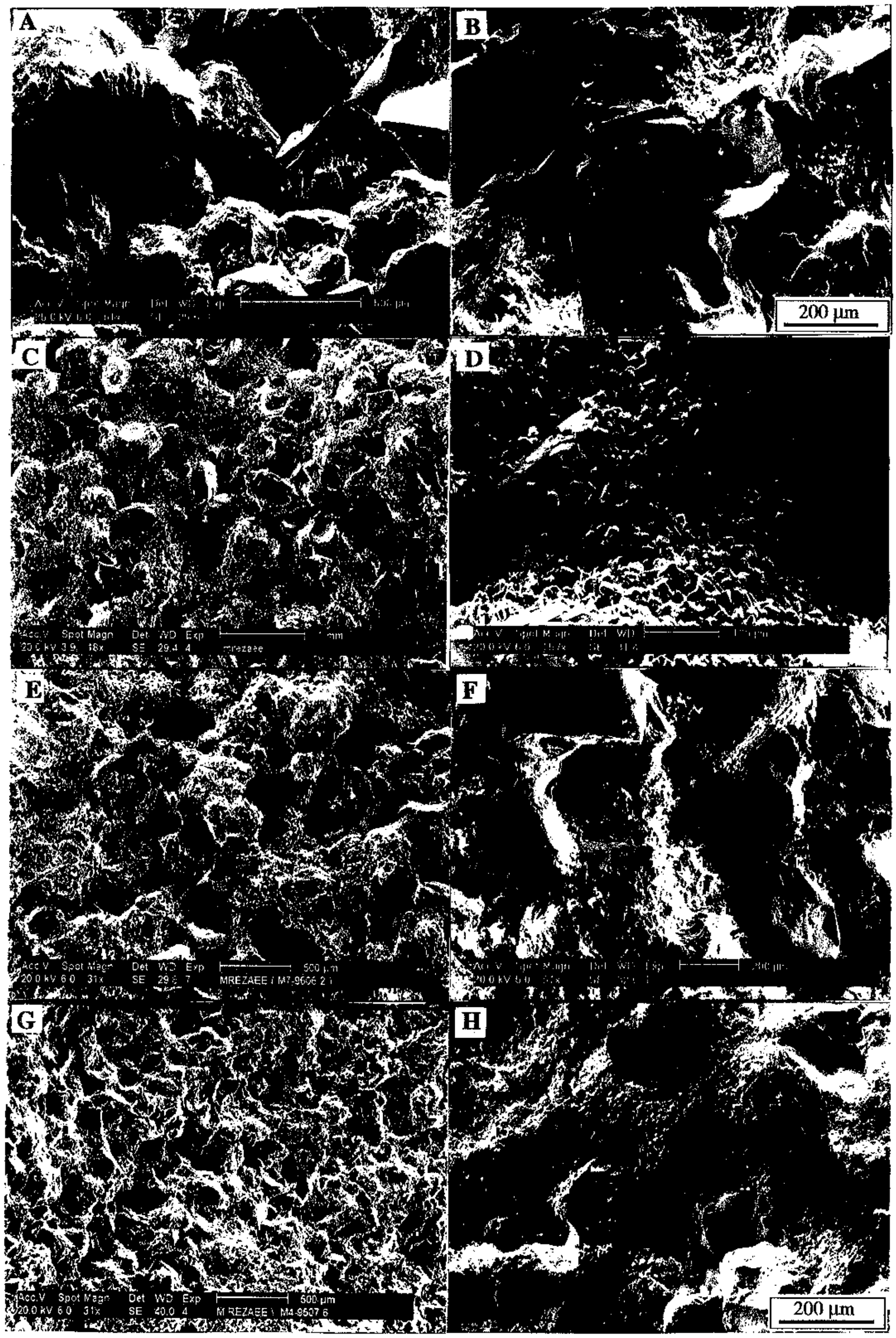

Fig. 9a-h - SEM micrographs of the representative samples of class 5 (A & B), class 6 (C & D), class 7 (E & F) and class 8 (G & H) of the Tirrawarra Sandstone.

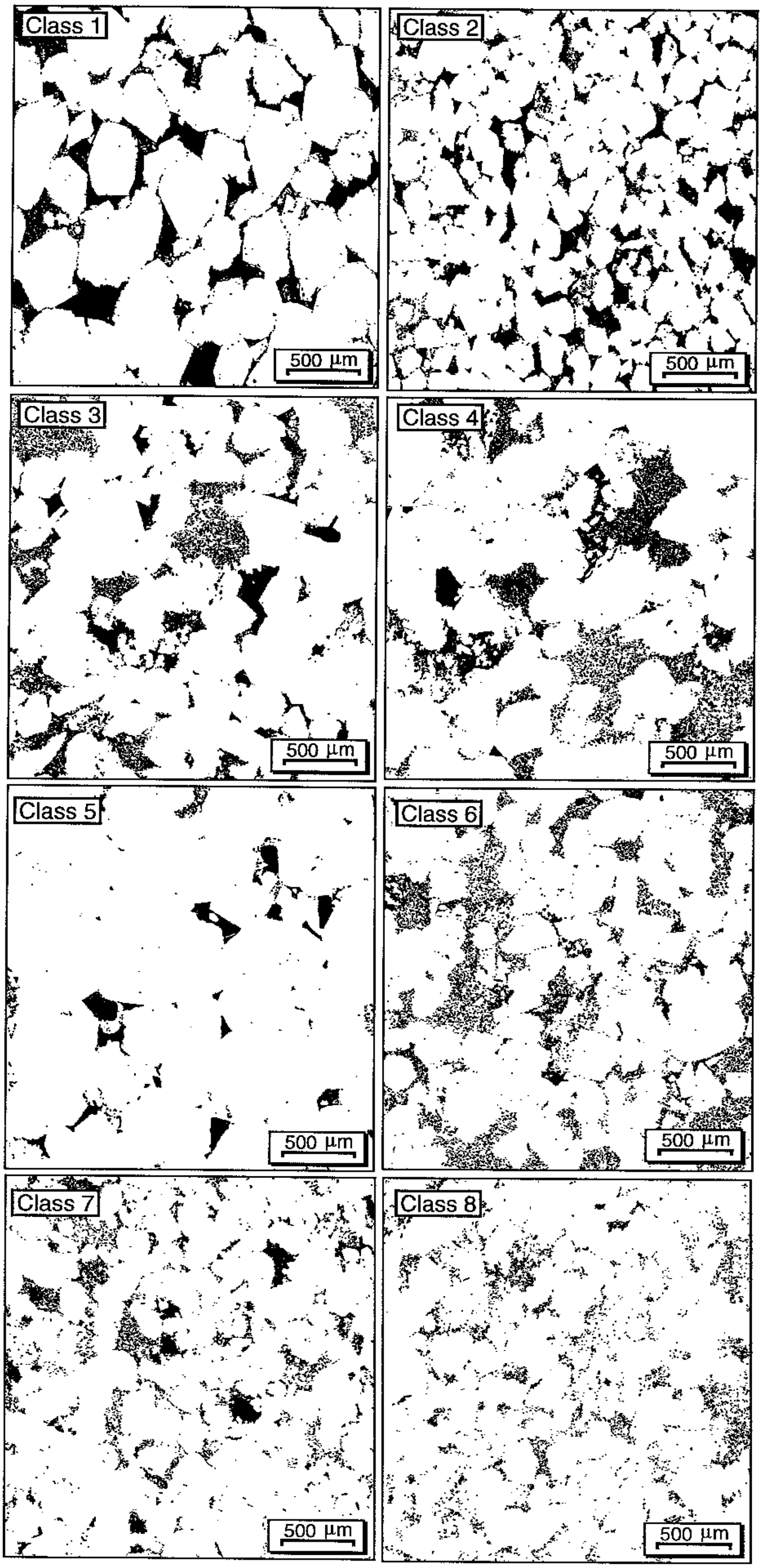

Fig. 10 - Binary images of representative samples of different reservoir classes from the Tirrawarra Sandstone.

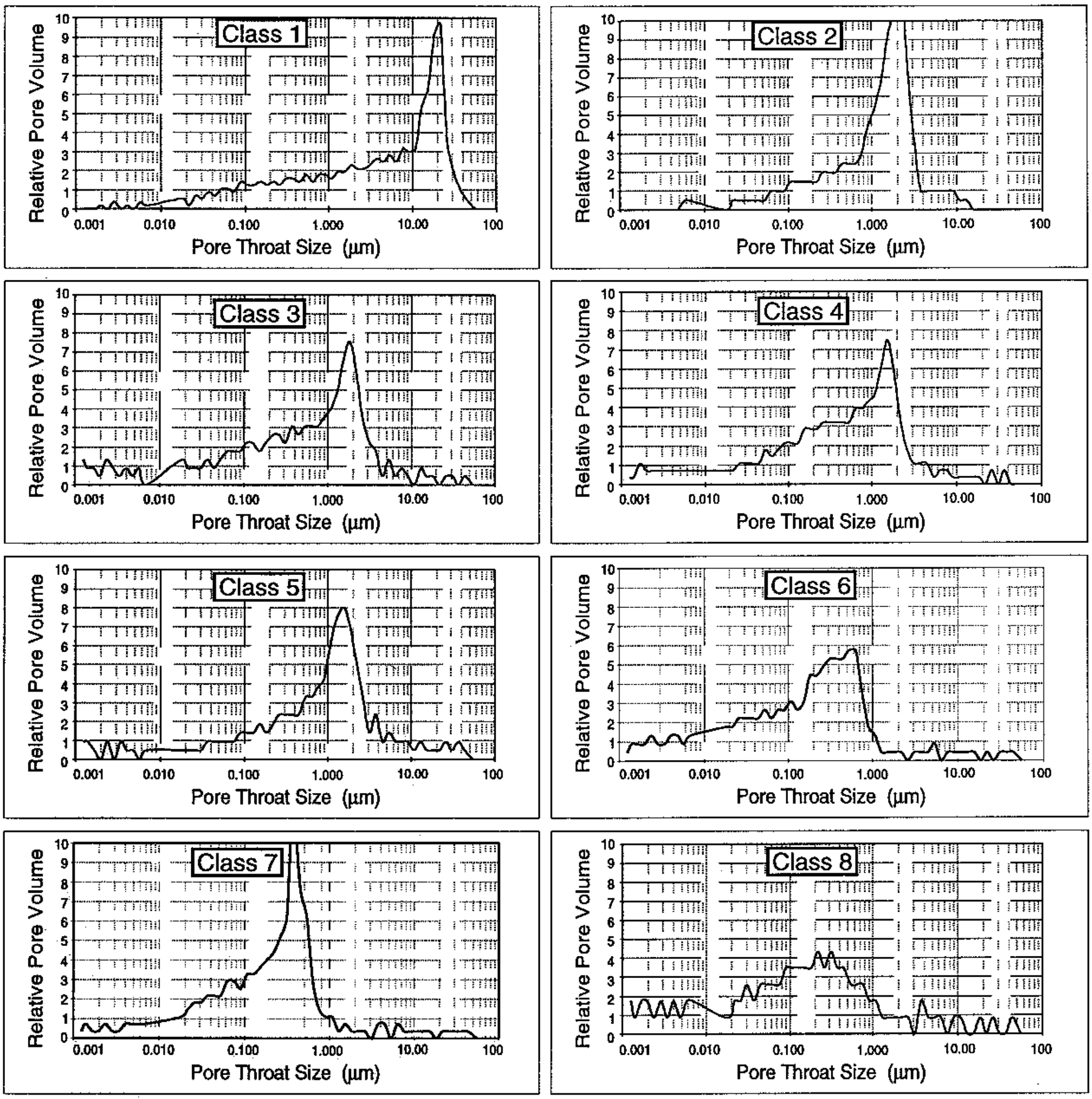

Fig. 11 - Pore throat size distribution.

permeability at the depositional surface. Porosity and permeability increase as sorting improves and grain size increases (Beard and Weyl, 1973; Pryor, 1973). Grain size and sorting of the samples belonging to the different sedimentary environments of the Tirrawarra Sandstone show a wide spectrum. In general, grain size from the medial part of the braid-delta decreases toward the aeolian environment (Fig. 16), whereas sorting improves from the medial part of braid-delta toward the aeolian environment (Fig. 17). Original intergranular volume (IGVo) which depends on grain size and sorting, varies in each sedimentary environment. IGVo decreases from the aeolian and meandering environments towards the medial braid-delta (Fig. 18). This reduction is not very pronounced in comparison with the reduction in the present intergranular volume (IGV) (Fig. 19). This means that in the Tirrawarra Sandstone, textural factors had no significant effect on the IGV and subsequently had no significant influence on pore geometry after deposition of sediments.

2 - Compostional characteristics

In the Tirrawarra Sandstone, the composition of sands varies significantly in different sedimentary environments. In general, the amount of rock fragments, which are mostly ductile, increases from the aeolian environment toward the braid-delta system (Fig. 20). Each environment therefore has its own set of compositional characteristics which, from

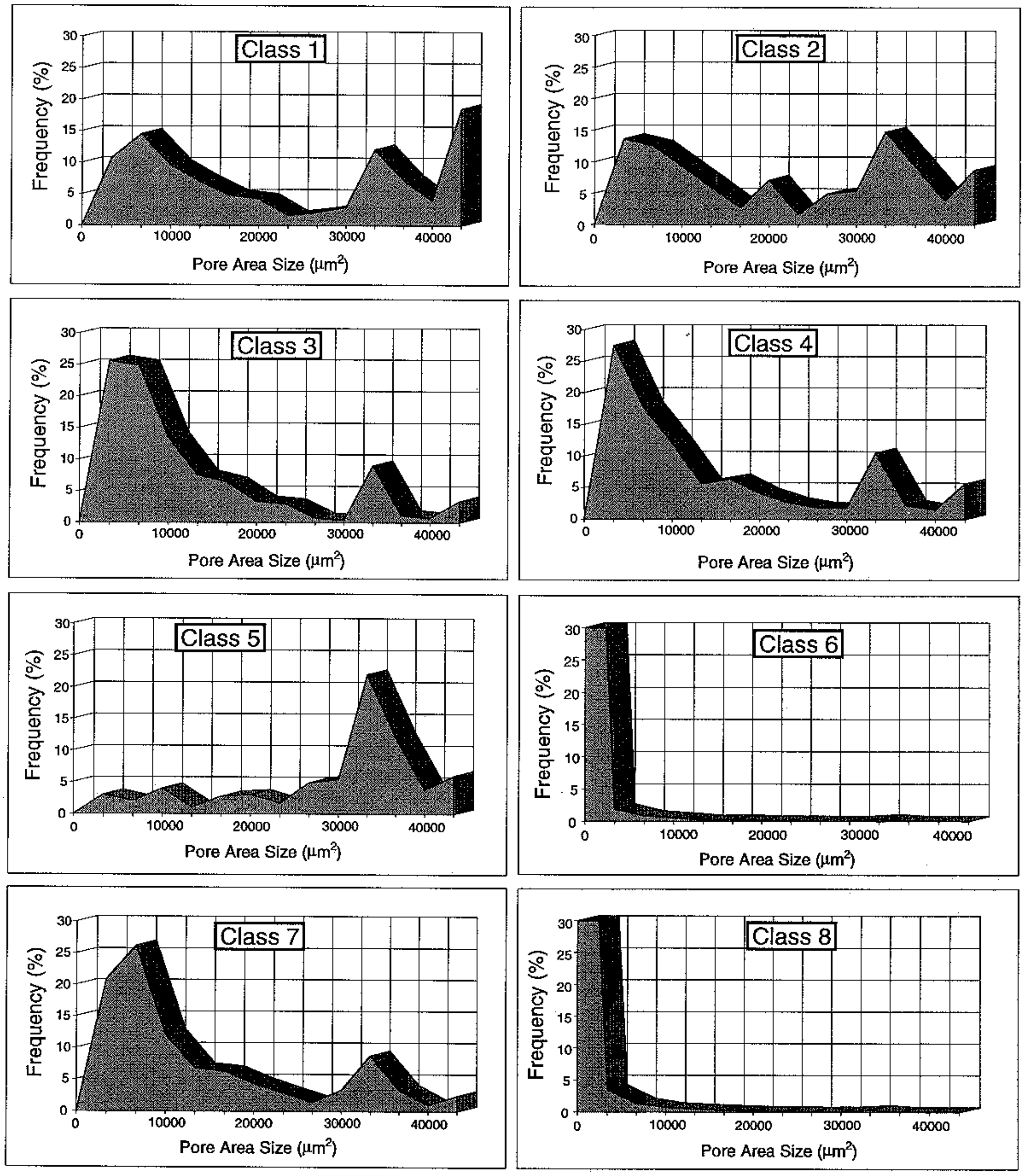

Fig. 12 - Mean pore area sizes of different classes from the Tirrawarra Sandstone.

the aeolian to the braid system, changes from dominantly quartz arenite to dominantly litharenite (Folk, 1974) (Fig. 4). In the Tirrawarra Sandstone, composition has a significant impact on subsequent diagenetic events. Compaction and quartz cementation are two major diagenetic events which significantly affected the pore spaces. The intensity of mechanical compaction shows a strong relationship with the composition of the sandstones. As the amount of rock fragments increases, the magnitude of compaction increases (Fig. 7). Several factors arise from the presence of ductile rock fragments which induce greater compaction in the samples.

- Quartz cement does not develop at a quartz to rock fragment contact, whereas at a quartz-quartz contact, even in the same sample, development of a thick overgrowth can occur. As the percentage of rock fragments increases, the development of quartz cement between the grains decreases (Fig. 5). The corollary of this is that quartz cementation increases with an increase of quartz grains. The development of early quartz cement spreads overburden pressure over a wider area of each grain, thereby inhibiting subsequent compaction.

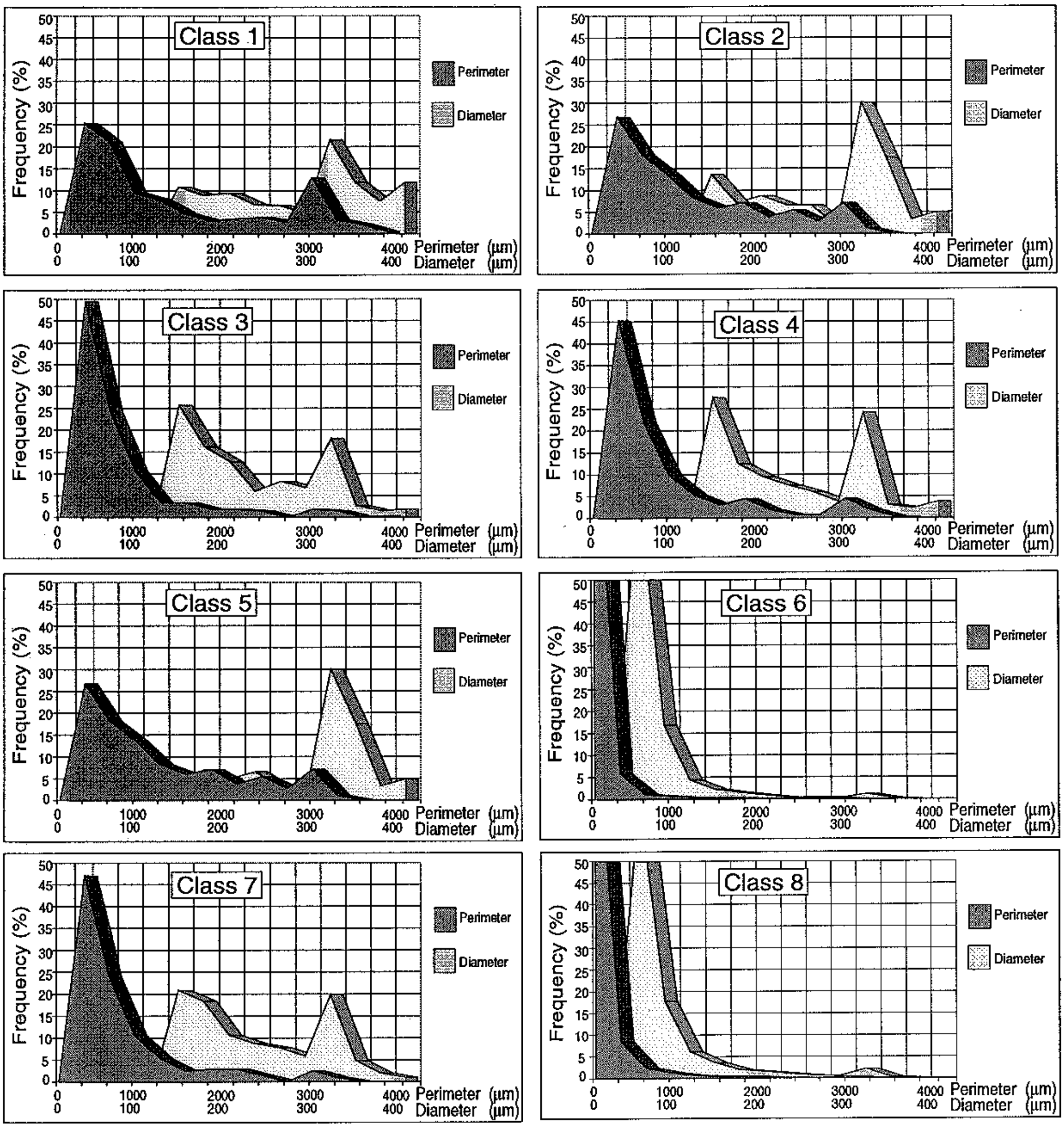

Fig. 13 - Mean pore diameter and mean pore perimeter sizes of different classes from the Tirrawarra Sandstone.

- Ductile rock fragments, especially metamorphic rock fragments such as mica schist and phyllite, can be readily deformed to pseudomatrix (Nagtegaal,1978), leading to occlusion of pore spaces and the sealing of pore throats.

Thin-section and SEM observations show that intergranular pores in quartz-rich samples with early quartz cement and subsequently with less compaction are preserved, and relatively good connectivity exists among the pores. With increasing amounts of rock fragments in the samples, pore space decreases and pore throat occlusion increases, mostly by plastic deformation of rock fragments.

It is concluded that, in the Tirrawarra Sandstone, depositional environments control sandstone composition, and sandstone composition controls compaction and cementation. In quartz-rich depositional facies, such as aeolian and meandering systems, compaction is slight and quartz cementation is relatively extensive, with widespread preservation of primary pore spaces and pore throats. On the other hand, in the braid-delta environment which is rich in rock fragments, mechanical compaction is greater and subsequently most of the intergranular primary porosity is lost and pore throats are sealed by plastic deformation of ductile rock fragments.

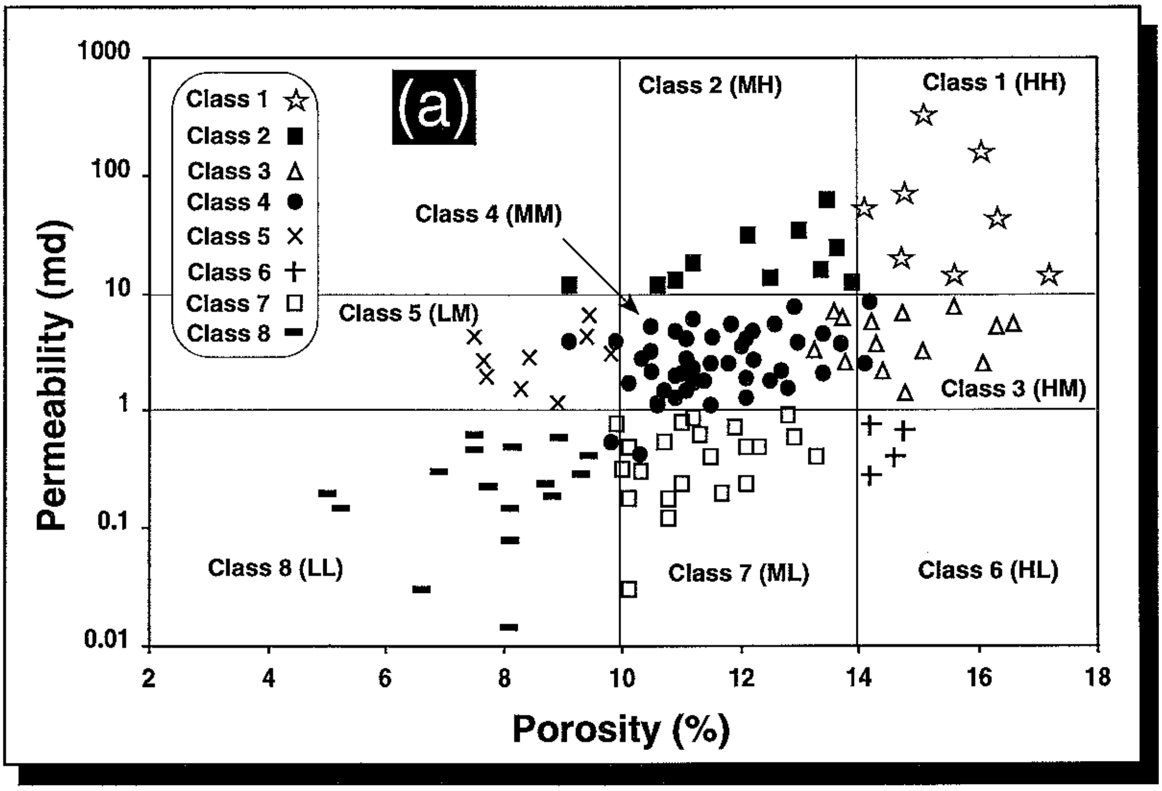

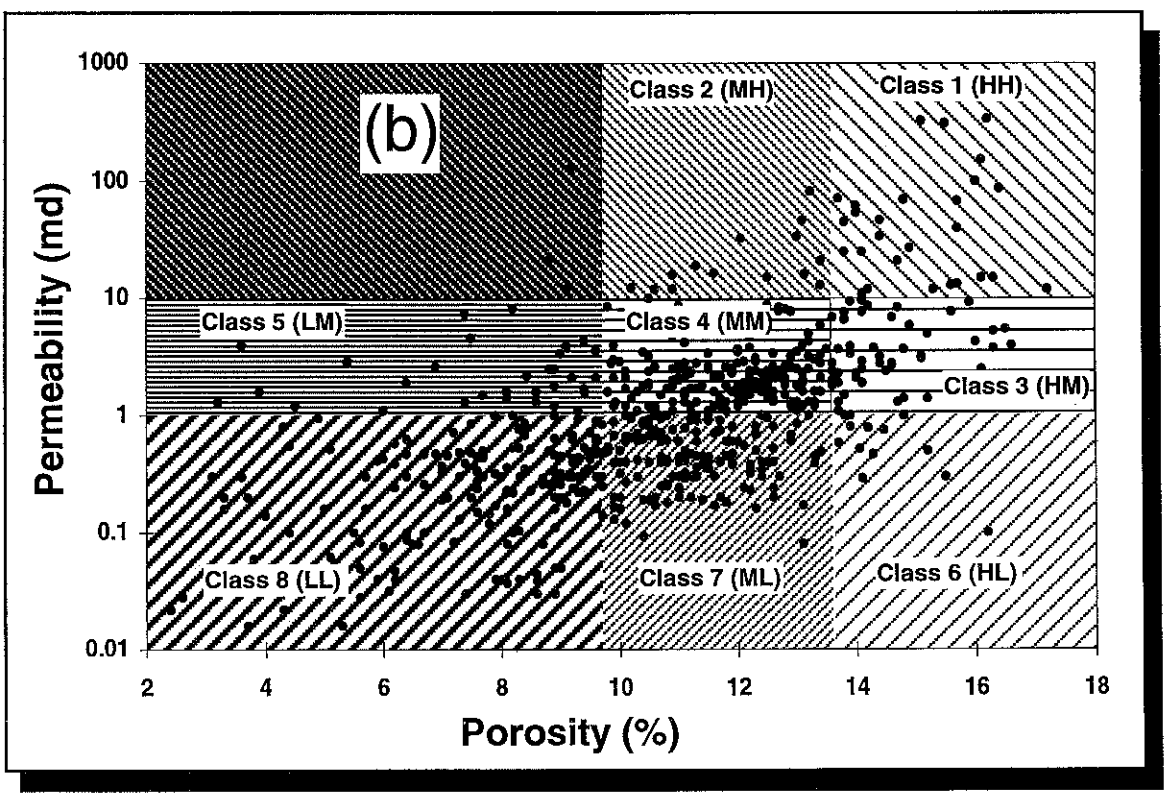

Fig. 14a-b - a) Semi-log cross-plots of porosity versus permeability for the studied samples. b) Semi-log cross-plot of porosity versus permeability of about 500 Tirrawarra Sandstone samples in the eight reservoir classes.

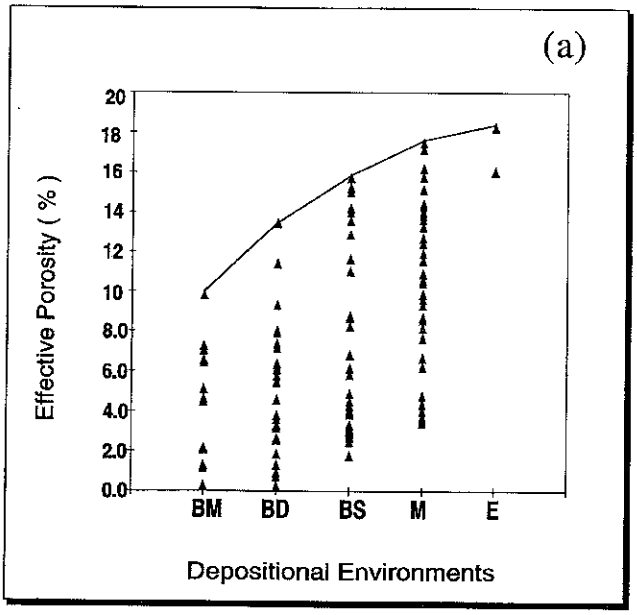

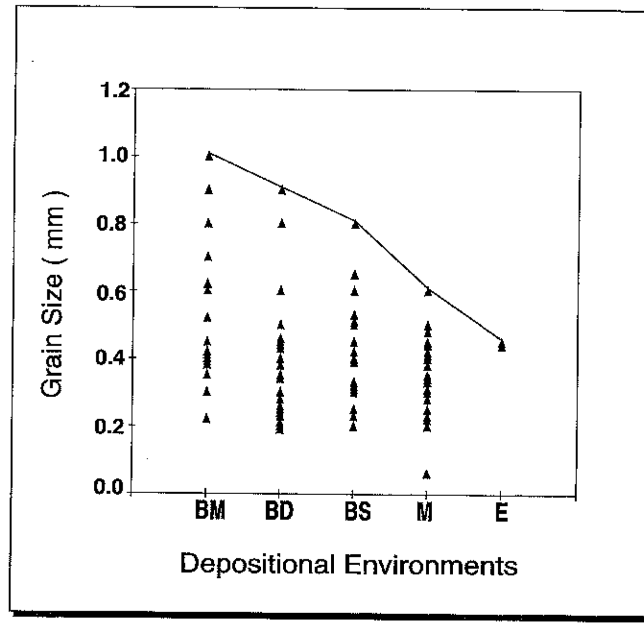

Fig. 16 - Cross-plot of depositional environment versus grain size. Environments as in Figure 15.

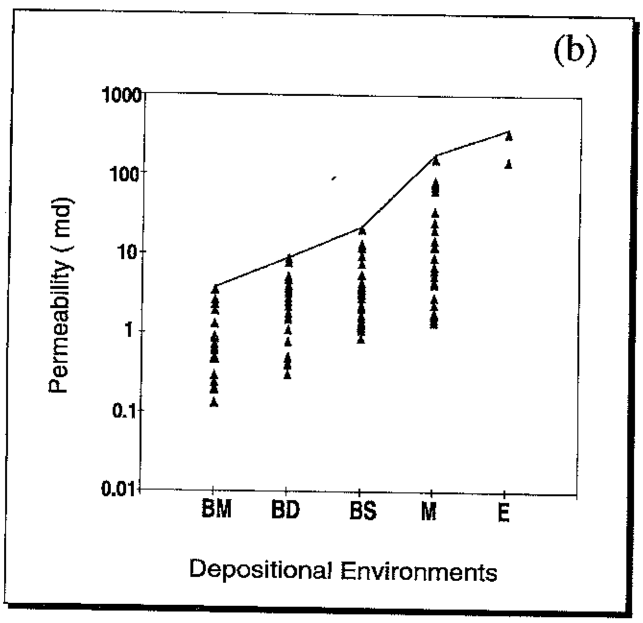

Fig. 15a-b - a) Cross-plot of depositional environment versus point count porosity (%). b) Semi-log cross plot of depositional environment versus permeability (mD). BM= medial part of the braid-delta, BD= distal part of the braid-delta, BS= beach barrier, M= meandering system and E= aeolian.

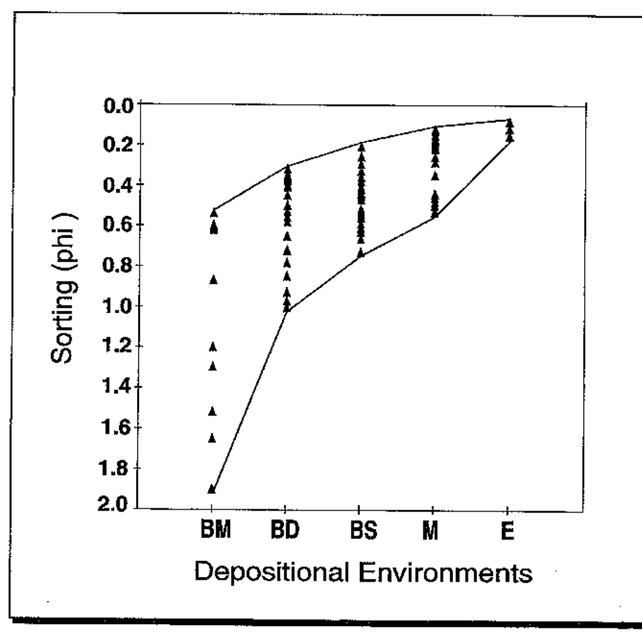

Fig. 17 - Cross-plot of depositional environment versus sorting. Environments as in Figure 15.

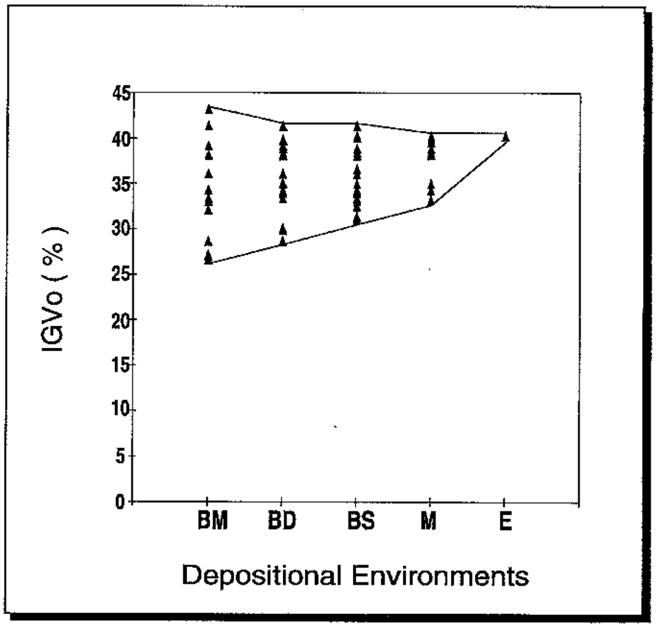

Fig. 18 - Cross-plot of depositional environment versus original intergranular volume (IGVo). Environments as in Figure 15.

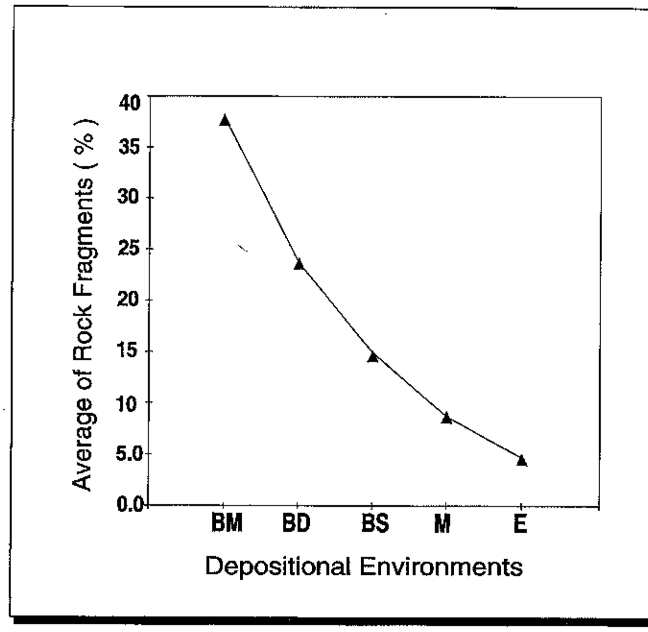

Fig. 20 - Cross-plot of depositional environment versus average of rock fragment percentage (%). Environments as in Figure 15.

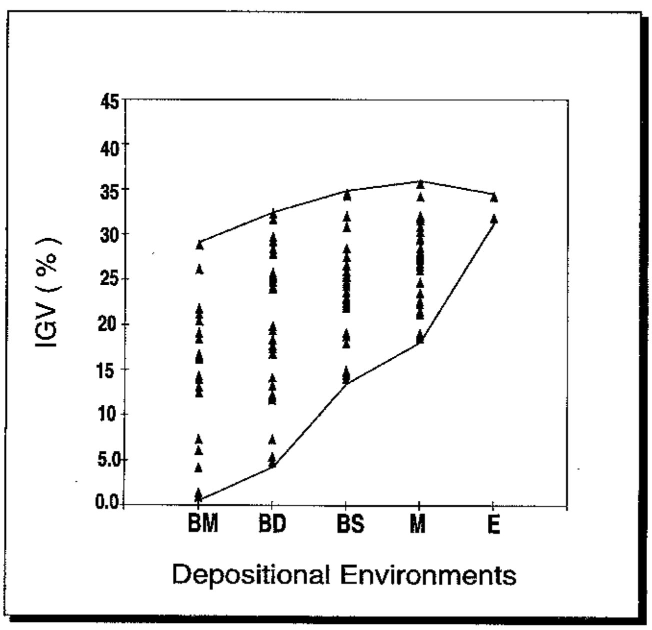

Fig. 19 - Cross-plot of depositional environment versus intergranular volume (IGV). Environments as in Figure 15.

Pore geometry control on the porosity and permeability

The cross-plot of porosity and permeability (Fig. 14a) does not show a straight and tight trend and the plotted data are very scattered. For example, permeability of samples with 10 per cent porosity ranges from 0.1 to more than 10 mD. This indicates that the amount of porosity is not the only factor which controls permeability and it is more likely that pore geometry is the principal parameter which controls permeability. In Figures 14a-b, the area with relatively high porosity and high permeability (HH) is defined by Class 1 samples which have the biggest pore area, pore diameter and pore throat sizes while the area with relatively low permeability and low porosity contains the Class 8 samples which have the smallest pore area, pore diameter and pore throat sizes. Pore and pore throat characteristics have a great influence on the permeability and porosity of the Tirrawarra Sandstones. Pore throat sizes decrease in a regular manner from Class 1 to Class 8 (Fig. 21) with a consequent decrease in permeability although pore area and pore diameter do not vary in the same regular way. An increase in pore area and pore diameter does not necessarily lead to an increase in permeability due to the presence of large secondary macroporosity.

One application of this study is the prediction of pore geometry and porosity type from core data. In Figure 14a, the samples of each class show a distinct range of porosity and permeability and, as each class indicates a particular pore geometry and pore throat size, it is possible to predict pore geometry of unknown samples with the knowledge of core analysis data (Fig. 14b).

Acknowledgements

We gratefully acknowledge financial support by NCPGG and SANTOS Ltd. The paper was greatly improved by the comments of PESA Journal reviewers, P. Baillie and K. Martin. The authors wish to acknowledge SANTOS Ltd (operator on behalf of the Cooper Basin consortium) for permission to present this paper.

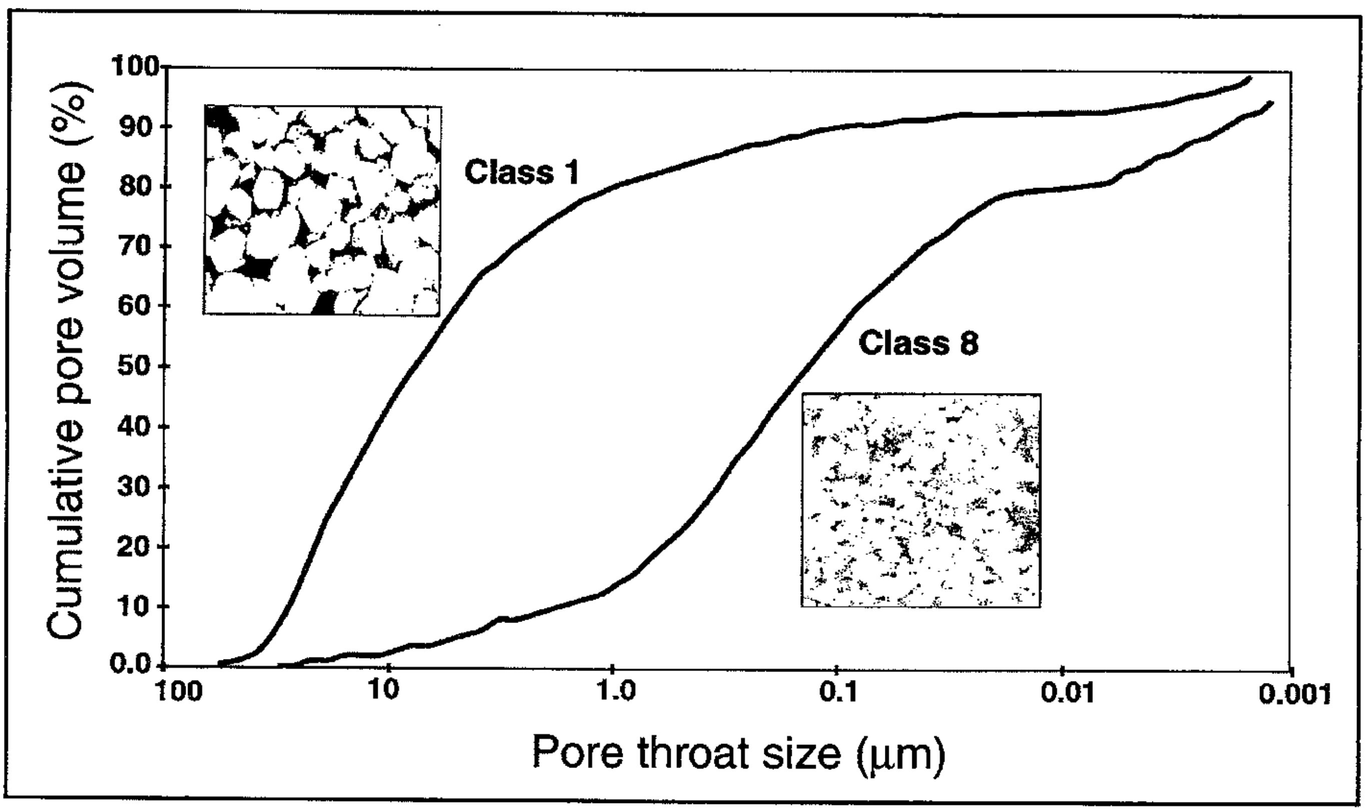

Fig. 21 - Comparison between the pore throat curves of representative samples of classes 1 and 8.

References

Apak, S.N. & Stuart, W.J. & Lemon, N.M., 1993. Structural-stratigraphic development of the Gidgealpa-Merrimelia-Innamincka Trend with implications for petroleum trap styles, Cooper Basin, Australia. APEA Journal, 33, 94-104.

Armstrong, J.D. & Barr, T.M., 1986. The Eromanga Basin. An overview of exploration and potential. Geological Society of Australian Special Publication, 12, 25-38.

Battersby, D.G., 1976. Cooper Basin oil and gas fields. *In:* Leslie, R. B. Evans, H. J. & Knight, C. L. (eds). Economic Geology of Australia and New Guinea, 3, Petroleum. Australasian Institute of Mining Metallurgy, Monograph, 7, 321-370.

Beard, D. C., & Weyl, P. K. 1973. Influence of texture on porosity and permeability of unconsolidated sand. AAPG Bull., 57, 349-369.

Ehrenberg, S.N. & Boassen, T. 1993. Factor controlling permeability variation in sandstones of the Garn Formation in Trestakk Field, Norwegian continental shelf. Journal of Sedimentary Petrology, 63, 929-944.

Ehrlich, R. Crabtree, S. J. Horkowitz, K. O. & Horkowitz, J. P. 1991. Petrography and reservoir physics I: Objective classification on reservoir porosity. AAPG Bull., 75, 1574-1562.

Ehrlich, R. Kennedy, S. K. Crabtree, S. J. & Cannon, R. L. 1984 Petrographic image analysis, I. analysis of reservoir pore complexes. Journal of Sedimentary Petrology, 54, 1365-1378.

Exon, N.F. & Senior, B. R. 1976. The Cretaceous of the Eromanga and Surat Basins. BMR Journal of Australian Geology and Geophysics, 1, 33-50.

Fairburn, W. A. 1989. The geometry of Toolachee unit 'C' fluvial sand trends, Moomba Field, Permian Cooper Basin, South Australia. APEA Journal, 29, 239-250.

Farrow, B. B. 1989. Permeability estimation from well logs using probabilities: The Cooper and Eromanga Basins, Australia. *In:* O'Neil, B.J. (ed.), Proceedings of the Cooper and Eromanga Basins conference, PESA, SPE and ASEG, Adelaide, 165-171.

Folk, R. L. 1974. Petrology of sedimentary rocks. Austin, Texas, Hemphill Publishing Co., 182p.

Gatehouse, C. G. 1972. Formations of the Gidgealpa Group in the Cooper Basin. Australasian Oil & Gas Review, 18, 10-15.

Gatehouse, C. G.,1986. The geology of the Warburton Basin in South Australia. Australian Journal of Earth Science, 33, 161-180.

Haszeldine, R.S. & Osborne, M. 1993. Fluid inclusion temperatures in diagenetic quartz reset by burial: implications for oil field cementation. *In:* Horbury, A. D. & Robinson, A. G. (eds). Diagenesis and Basin Development by AAPG Studies in Geology, 36, 35-46.

Heath, R., 1989. Exploration in the Cooper Basin. APEA Journal, 29, 366-378.

Hunt, J.W., Heath, R.S. & McKenzie, P.F. 1989. Thermal maturity and other geological controls on the distribution and composition of Cooper Basin hydrocarbons. *In:* O'Neil B.J. (ed). The Cooper and Eromanga Basins, Australia. Proceedings of the Cooper and Eromanga Basins Conference, PESA, SPE, ASEG, Adelaide, p.509-523.

Kantsler, A.J., Prudence, T.J.C., Cook, A.C. & Zwigulis, M. 1983. Hydrocarbon habitat of the Cooper/Eromanga Basin. APEA Journal, 23, 373-389.

Kapel, A.J. 1966. The Cooper's Creek Basin. APEA Journal, 6, 71-75.

Kapel, A.J., 1972. The geology of the Patchawarra area Cooper Basin. APEA Journal, 12., p.53-57.

McCreesh, C.A., Ehrlich, R. & Crabtree, S.J. 1991. Petrography and reservoir physics II: Relating thin section porosity to capillary pressure, the association between pore types and throat size. AAPG Bull., 75, 1563-1578.

Nagtegaal, P.J.C. 1978. Sandstone framework instability as a function of burial diagenesis. Journal of Geological Society of London, 135, 101-105.

Osborne, M. & Haszeldine, R.S. 1993. Fluid inclusions in diagenetic quartz record oilfield burial temperatures, not precipitation temperatures. Marine and Petroleum Geology, 10.

Pittman, E.D. 1979. Porosity, diagenesis and productive capability of sandstone reservoirs. SEPM Special Publication, 26, 159-173.

Pittman, E.D. 1992. Relation of porosity and permeability to various parameters derived from mercury injection-capillary pressure curves for sandstones. AAPG Bull., 76, 191-198.

Pryor, W.A. 1973. Permeability-porosity patterns and variations in some Holocene sand bodies. AAPG Bull., 57, 162-189.

Purcell, W.R. 1949. Capillary pressure - their measurement using mercury and the calculation of permeability therefrom. AIME Petroleum Transactions, February 1949 p.39-48.

Rezaee, M.R., Lemon, N.M. & Seggie, R., 1997. Tectonic fingerprints in siderite cement, Tirrawarra Sandstone, southern Cooper Basin, South Australia. Geological Magazine, vol. 133, no. 7.

Rezaee, M.R. & Lemon, N.M., 1996. Influence of depositional environment on diagenesis and reservoir quality: Tirrawarra Sandstone reservoir, southern Cooper Basin, Australia. Journal of Petroleum Geology, vol. 19, 269-391.

Rezaee, M.R. & Schulz-Rojahn, J. P., 1996. Application of quantitative back-scattered electron image analysis in isotope interpretation of siderite cement: Tirrawarra Sandstone reservoir, Cooper Basin (Australia), *In:* Morad, S. (ed.), Carbonate cementation in sandstones: International Association of Sedimentologists Special Publication, in press.

Rezaee, M.R. & Tingate, P.R., 1996. Precipitation temperatures and origin of quartz cement and its influence on the Tirrawarra Sandstone reservoir quality, southern Cooper Basin, South Australia. Geological Society Of Australia, Abstract No.41, p.362. 13th Australian Geological Convention, Canberra, February, 1996.

Rezaee, M.R. & Tingate, P.R., 1997. Origin of the quartz cement, Tirrawarra Sandstone, Southern Cooper Basin, South Australia. Journal of Sedimentary Research, in vol. 67, p. 168-177.

Rodda, J.S. & Paspaliaris T.G., 1989. Tirrawarra and Moorari Oil Fields enhanced oil recovery schemes - further developments. APEA Journal, 29, 121-130.

Schulz-Rojahn, J.P., & Phillips, S.E., 1989. Diagenetic alteration of Permian reservoir sandstones in the Nappamerri Trough and adjacent areas, southern Cooper Basin. *In:* O'Neil, B. J., (ed.), The Cooper and Eromanga Basin, Australia. Proceedings of the Petroleum Exploration Society of Australia, Society of Petroleum Engineers, Australian Society of Exploration Geophysics, 629-645.

Seggie, R.J., Lansom, P.B., Hamlin, H.S. & Johnson, G. A., 1994. The Tirrawarra Oil Field: Field revitalisation through reservoir description and characterisation: APEA Journal, 34, 33-54.

Senior, B.R., Mond, A. & Harrison, P.L. 1978. Geology of the Eromanga Basin. BMR Bull., 167, 102p.

Smyth, M. 1979. Hydrocarbon generation in the Fly Lake-Brolga area of the Cooper Basin. APEA Journal, 19, 108-114.

Stuart, W.J. 1976. The genesis of Permian and Lower Triassic reservoir sandstones during phases of southern Cooper Basin development. APEA Journal, 16, 37-47.

Stuart, W.J. & Farrow, B.B. Lemon, N.M. & Phillips, S.E. 1990. Porosity and permeability in Permian sandstones: southern Cooper Basin. Final report, NERDDC Project No. 1175, National Centre for Petroleum Geology & Geophysics, University of Adelaide, Australia. 104p.

Stuart, W.J. & Kennedy, S. & Thomas, A.D., 1988. Influence of structural growth and other factors on the configuration of fluviatile sandstones, Permian Cooper Basin. APEA Journal, 28, 255-265.

Thornton, R.C.N., 1979. Regional stratigraphic analysis of the Gidgealpa Group, Southern Cooper Basin, Australia. Geological Survey of South Australia Bull., 49.

Tingate, P.R. & Luo, P., 1992. Silica diagenesis and pore development in Permian sandstones, southern Cooper Basin. APEA Journal, 32, 325-338.

Wardlaw, N.C., 1979. Pore geometry of carbonate rocks as revealed by pore casts and capillary pressure. AAPG Bull., 60, 245-257.

Williams, B.P.J. Wild, E.K. & Suttill, R.J. 1985. Paraglacial aeolianites: potential new hydrocarbon reservoirs, Gidgealpa Group, southern Cooper Basin. APEA Journal, 25, 291-310.

Yew, C.C. & Mills, A. A., 1989. The occurrence and search for Permian oil in the Cooper Basin, Australia. *In:* O'Neil B.J. (ed.) The Cooper and Eromanga Basins, Australia. (Proceedings of the Cooper and Eromanga Basins Conference, PESA, SPE, ASEG Adelaide, 339-359.